

Botulinum Neurotoxin Type B Uses a Distinct Entry Pathway Mediated By Cdc42 Into Intestinal Cells Versus Neuronal Cells.

Chloé Connan, Marie Voillequin, Carolina Varela Chavez, Christelle Mazuet, Christian Leveque, Sandrine Vitry, Alain Vandewalle, Michel R Popoff

▶ **To cite this version:**

Chloé Connan, Marie Voillequin, Carolina Varela Chavez, Christelle Mazuet, Christian Leveque, et al.. Botulinum Neurotoxin Type B Uses a Distinct Entry Pathway Mediated By Cdc42 Into Intestinal Cells Versus Neuronal Cells.. Cellular Microbiology, 2017, 10.1111/cmi.12738 . pasteur-01493360

HAL Id: pasteur-01493360

https://pasteur.hal.science/pasteur-01493360

Submitted on 21 Mar 2017

HAL is a multi-disciplinary open access archive for the deposit and dissemination of scientific research documents, whether they are published or not. The documents may come from teaching and research institutions in France or abroad, or from public or private research centers.

L'archive ouverte pluridisciplinaire **HAL**, est destinée au dépôt et à la diffusion de documents scientifiques de niveau recherche, publiés ou non, émanant des établissements d'enseignement et de recherche français ou étrangers, des laboratoires publics ou privés.



Distributed under a Creative Commons Attribution - NonCommercial 4.0 International License

REVISED

BOTULINUM NEUROTOXIN TYPE B USES A DISTINCT ENTRY PATHWAY MEDIATED BY CDC42 INTO INTESTINAL CELLS VERSUS NEURONAL CELLS

Chloé CONNAN[1], Marie VOILLEQUIN[1], Carolina VARELA CHAVEZ[1], Christelle MAZUET[1], Christian LEVEQUE[2], Sandrine VITRY[3], Alain VANDEWALLE[4], Michel R. POPOFF[1*]

[1] Bactéries anaérobies et Toxines, Institut Pasteur, 75015 Paris, France

[2] INSERM, UMR_S 1072 (UNIS), Faculté de Médecine -Secteur Nord, Aix Marseille Université, 13015 Marseille, France

[3] Neuro-Immunologie Virale, Institut Pasteur, 75015 Paris, France

[4] UMRS1149, Université Paris 7-Denis Diderot, 75018 Paris, France

Short title: *Botulinum* neurotoxin B entry into intestinal cells

Key words: *Clostridium botulinum*, botulinum neurotoxin, endocytosis, intestinal cells, neuronal cells, Cdc42, gangliosides.

Accepted Article

This article has been accepted for publication and undergone full peer review but has not been through the copyediting, typesetting, pagination and proofreading process which may lead to differences between this version and the Version of Record. Please cite this article as doi: 10.1111/cmi.12738

ABSTRACT

Botulinum neurotoxins (BoNTs) are responsible for severe flaccid paralysis by inhibiting the release of acetylcholine at the neuromuscular junctions. BoNT/B most often induces mild forms of botulism with predominant dysautonomic symptoms. In food borne botulism and botulism by intestinal colonization such as infant botulism, which are the most frequent naturally acquired forms of botulism, the digestive tract is the main entry route of BoNTs into the organism. We previously showed that BoNT/B translocates through mouse intestinal barrier by an endocytosis-dependent mechanism and subsequently targets neuronal cells, mainly cholinergic neurons, in the intestinal mucosa and musculosa. Here we investigated the entry pathway of BoNT/B using fluorescent C-terminal domain of the heavy chain (HcB) which is involved in the binding to specific receptor(s) and entry process into target cells. While the combination of gangliosides $GD_{1a}/GD_{1b}/GT_{1b}$ and synaptotagmin I and to a greater extent synaptotagmin II constitutes the functional HcB receptor on NG108-15 neuronal cells, HcB only uses the gangliosides $GD_{1a}/GD_{1b}/GT_{1b}$ to efficiently bind to m-IC_{cl2} intestinal cells. HcB enters both cell types by a dynamin-dependent endocytosis which is efficiently prevented by Dynasore, a dynamin inhibitor, and reaches a common early endosomal compartment labeled by EEA1. In contrast to neuronal cells, HcB uses a Cdc42-dependent pathway to enter intestinal cells. Then, HcB is transported to late endosomes in neuronal cells, whereas it exploits a non-acidified pathway from apical to basal lateral side of m-IC_{cl2} cells supporting a transcytotic route in epithelial intestinal cells.

Accepted Article

This article is protected by copyright. All rights reserved.

INTRODUCTION

Botulinum neurotoxins (BoNTs) are potent toxins that inhibit the release of spontaneous and nerve evoked neurotransmitters and more specially the release of acetylcholine (Ach) at the neuro-muscular junctions and other cholinergic endings of the peripheral nervous system. Botulism results in a flaccid paralysis and reduction of secretions which lead to skeletal muscle paralysis, respiratory insufficiency, and death in the most severe forms (Sobel, 2005, Poulain *et al.*, 2008). BoNTs are divided into seven toxinotypes (A to G) according to their immunological properties and in numerous subtypes based on amino acid sequence variations (Hill *et al.*, 2013, Peck *et al.*, 2017). A new BoNT type called H has been reported but was characterized as an A/F hybrid (Barash *et al.*, 2014, Maslanka *et al.*, 2016). In natural conditions, botulism is acquired by ingestion of preformed BoNT in food (foodborne botulism), or after intestinal or more rarely wound colonization and subsequent *in situ* BoNT production (Sobel, 2005). Indeed, *C. botulinum* can contaminate and synthesize BoNT in foods, and under certain circumstances this bacterium can grow and produce toxin in the intestine. This is the case in babies and young children (infant botulism) or in adults with predisposing factors such as intestinal surgery, antibiotherapy, chronic inflammation, necrotic lesions of the intestinal mucosa, and anatomical or functional abnormalities of the intestine. An immaturity or perturbation of the resident intestinal microbiota seems to be the main factor which facilitates the implantation of *C. botulinum* in the digestive tract (Arnon, 1989, Fox *et al.*, 2005, Brook, 2007, Fenicia *et al.*, 2009, Rosow *et al.*, 2015). Therefore, most often the digestive tract represents the entry pathway for botulism. In food intoxication and during intestinal colonization with *C. botulinum*, the ingested or locally produced BoNT has to cross the digestive tract epithelium prior to have access to the target neurons.

BoNT/B is commonly associated with numerous cases of food borne botulism or infant botulism in humans throughout the world (Sobel, 2005, Popoff *et al.*, 2013). Although all BoNT types induce a descending flaccid paralysis, differences in the clinical picture have been observed according to the BoNT type. Thereby, type B botulism is more often less severe and less lasting than type A botulism (Woodruff *et al.*, 1992, Cherington, 1998). Dysautonomia (diplopia, blurred vision, dry mouth, dysphagia, constipation) is more frequent, and the motor symptoms are less pronounced in type B botulism than in type A (Hughes *et al.*, 1981, Merz *et al.*, 2003, Potulska-Chromik *et al.*, 2013). BoNT/B seems to have a higher affinity to cholinergic autonomic than motor-neuron endings (Brashear *et al.*, 1999). BoNT/B and BoNT/A recognize distinct receptors on neuronal cells, synaptotagmin

This article is protected by copyright. All rights reserved.

(Syt) and synaptic vesicle (SV2) protein, respectively, which might account for the differential recognition of neurons by the two toxins (review in (Rummel, 2013)). In addition, BoNT/B and BoNT/A might use distinct trafficking pathways or mode of dissemination from the digestive tract to the target neurons.

BoNTs associate with non-toxin proteins (ANTPs) produced by *C. botulinum* to form complexes of variable sizes (300 to 900 kDa). ANTPs encompass a non-toxic and non-hemagglutinin component (NTNH), and either several hemagglutinin components (HAs) or other non-hemagglutinin proteins called OrfX1, OrfX2, OrfX3 or P47 (Oguma *et al.*, 1999, Popoff *et al.*, 1999, Quinn *et al.*, 2001, Sharma *et al.*, 2003). One of the main role of ANTPs is to protect BoNT from degradation by the stomach acidic pH and digestive proteases. Indeed, NTNH retains a similar structure than that of BoNT and assembles with BoNT forming a compact interlocked complex resistant to acidic pH and protease degradation (Gu *et al.*, 2012, Inui *et al.*, 2012, Sagane *et al.*, 2012). The mode of passage of either BoNT alone or the whole BoNT complexes through the intestinal epithelial barrier is still controversial. HA complexes, but not OrfX proteins, have been shown to bind to epithelial cadherin (E-cadherin) and to disrupt the intercellular junctional complexes between epithelial cells thus facilitating the passage of BoNT complexes through epithelial barrier by the paracellular way (Jin *et al.*, 2009, Sugawara *et al.*, 2010, Sugawara *et al.*, 2011, Lee *et al.*, 2014, Lam *et al.*, 2015). However, it is not clear whether whole BoNT complex or BoNT alone is transported through the intestinal barrier. At acidic pH, BoNT complexes are highly stable, but at the neutral or basic pH of the duodenum and jejunum, BoNT complexes dissociate (review in (Poulain *et al.*, 2008). BoNTs alone have been reported to cross the intestinal barrier upon a transcytotic mechanism without the help of HAs or other ANTPs (Fujinaga *et al.*, 1997, Maksymowych *et al.*, 1998, Park *et al.*, 2003, Maksymowych *et al.*, 2004, Nishikawa *et al.*, 2004, Ahsan *et al.*, 2005, Couesnon *et al.*, 2008). Notably, we have shown that BoNT/B free of HAs is able to translocate through mouse intestinal barrier via an endocytosis-dependent process and rapidly targets in 10 min the enteric nervous system, mainly the cholinergic intestinal neurons (Connan *et al.*, 2016). These finding led us to investigate and compared the mode of BoNT/B entry into cell models of intestinal cell and neuronal cells.

RESULTS

HcB enters neuronal and intestinal cells

The C-terminal domain (Hc) of clostridial neurotoxin heavy chains is involved in the specific recognition and interaction with cell surface receptors. Hc has already extensively

This article is protected by copyright. All rights reserved.

been used to investigate internalization and intracellular trafficking of clostridial neurotoxins in cells as well as toxin translocation through the intestinal epithelium and dissemination in the subjacent tissues (Lalli *et al.*, 2003, Maksymowych *et al.*, 2004, Bohnert *et al.*, 2005, Roux *et al.*, 2006, Harper *et al.*, 2011, Restani *et al.*, 2012, Lam *et al.*, 2015). Notably, we used fluorescent Hc domains of BoNT/A and BoNT/B to analyze the neurotoxin passage and dissemination in mouse intestinal mucosa (Couesnon *et al.*, 2008, Connan *et al.*, 2016). Thereby, recombinant Hc from BoNT/B (HcB) labeled with Cy3 was used to monitor BoNT/B entry into cells. First, fluorescent HcB was incubated with several cell types at 37°C for 15 min. HcB nicely decorated the extensions and plasma membrane of primary rat cortical neurons and was visualized in intracellular compartments (Fig. 1). HcB-Cy3 also labeled the membrane of the neuronal cell line NG108-15, but to a lower extent than in primary neuronal cells. Primary neuronal cells likely retain a larger number of HcB receptors or higher affinity receptors compared to cultured neuronal or intestinal cell lines. When incubated at 37°C for 15 min, the largest part of HcB-Cy3 was localized in intracellular compartments indicating that HcB was efficiently internalized into the NG108-15 cell line (Fig. 1). In most cells, HcB-Cy3 was distributed in perinuclear compartments. Since HcB-Cy3 internalization was more easily monitored in NG108-15 cells due to the larger volume of NG108-15 versus that of primary neuronal cell bodies, NG108-15 cells were used in the subsequent experiments.

HcB-Cy3 entry was tested is several intestinal cell lines (CaCo-2, T84, mouse intestinal crypt cells (m-IC_{cl2})) with approximately the same efficiency (data not shown). m-IC_{cl2} were used as they were found to be a relevant model for analyzing the entry of BoNTs into intestinal cells (Couesnon *et al.*, 2008). After 15 min incubation, HcB was localized in intracellular compartments, which were more scattered through the cytoplasm than in neuronal cells (Fig. 1).

HcB-Cy3 entry was investigated in polarized m-IC_{cl2} cells grown on filters. HcB-Cy3 (2.5 µg/ml) was added in the apical chamber of the cell cultures which were incubated at 37°C for 3 min. Then, the cells were washed and further incubated with culture medium at 37°C for the indicated times (Fig. 2A and 2B). The HcB-Cy3 spots were monitored in the apical, center, and basolateral side of the polarized cells over time (Fig. 2B). Thus, a progressive passage of HcB-Cy3 was observed from apical brush border binding to basolateral endocytic compartments of m-IC_{cl2} cells within 10-20 min. HcB-Cy3 was also visualized in cultured NG108-15 over time (Fig. 2C and 2D). It is noteworthy that the

This article is protected by copyright. All rights reserved.

internalization level of HcB-Cy3 was lower in intestinal cells compared to neuronal cells (Fig. 2).

HcB enters neuronal and intestinal cells in a dynamin-dependent manner

BoNTs enter target cells via a receptor-mediated endocytosis (Beard, 2014, Rossetto *et al.*, 2014), but the precise mechanism of endocytosis according to the cell types is still elusive. BoNT/A has been found to enter neuronal and intestinal cells by a dynamin-dependent pathway in both cell types (Couesnon *et al.*, 2009). Dynasore, an inhibitor of dynamin-mediated endocytosis (Macia *et al.*, 2006) blocks BoNT/A entry into cultured hippocampal neurons (Harper *et al.*, 2011). Here, we investigated the inhibitory effect of Dynasore in the entry of HcB-Cy3 in neuronal and intestinal cells (Fig. 3). Cells were pretreated with Dynasore (80 μM) for 30 min and were then incubated with HcB-Cy3 for additional 10 min. As shown in Fig. 3A, Dynasore efficiently prevented HcB-Cy3 entry in both neuronal NG108-15 cells and intestinal crypt m-IC_{cl2} cells. However, HcB-Cy3 still decorated the plasma membrane of NG108-15 neuronal cells indicating that HcB binding to surface cell receptor was unaffected by Dynasore treatment. To further support the dynamin-dependent HcB-Cy3 entry into cells, NG108-15 and m-IC_{cl2} cells were transfected with the dominant negative dynamin2 K44A as previously described (Couesnon *et al.*, 2010) and then exposed to HcB-Cy3. Dynamin2 K44A prevented HcB-Cy3 internalization in both neuronal and intestinal cells (Sup. Fig. 1).

The HcB entry pathway in NG108-15 and m-IC_{cl2} was further investigated using potassium depletion followed by hypotonic shock which disrupts the formation of clathrin-coated vesicles and prevents clathrin-mediated endocytosis (Carpentier *et al.*, 1989, Kovbasnjuk *et al.*, 2001). HcB-Cy3 internalization was significantly prevented in NG108-15 pretreated in K+-depleted buffer. The fluorescent HcB molecules mainly decorated the cell periphery. In contrast, K+ depletion did not significantly alter the HcB-Cy3 entry into m-IC_{cl2} indicating that HcB mainly used a clathrin-mediated endocytosis in NG108-15 and an alternative pathway in m-IC_{cl2} cells (Fig. 4).

HcB uses gangliosides GD_{1a}, GD_{1b}, GT_{1b} but not GM1 as receptors on intestinal cells

The specific receptors of BoNT/B on neuronal cells have been identified as gangliosides GT1a, GD_{1b}, GT_{1b} associated to SytI and SytII (Nishiki *et al.*, 1994, Nishiki *et al.*, 1996a, Jin *et al.*, 2006, Rummel *et al.*, 2007). Does BoNT/B recognize the same receptors

This article is protected by copyright. All rights reserved.

on intestinal cells than on neuronal cells for its entry into epithelial cells? Gangliosides are components of plasma membrane of all cell types, but they are predominantly concentrated in nerve endings. Firstly, we investigated the role of gangliosides in HcB entry into neuronal and intestinal cells. Competition experiments were performed between HcB-Cy3 and gangliosides in m-IC_{cl2} cells versus NG108-15 cells. When HcB-Cy3 was preincubated with a preparation (gg) enriched in gangliosides GD_{1a}, GD_{1b}, and GT_{1b} (250 μg/ml), HcB-Cy3 internalization was strongly reduced in m-IC_{cl2} cells and to a lower extent in NG108-15 cells (Fig. 5). In contrast, GM1 (50 μg/ml) did not significantly impair the binding and entry of HcB-Cy3 into intestinal and neuronal cells (Fig. 5). GM1 was already reported to not be included in the BoNT/B receptor ganglioside moiety on neuronal cells (Nishiki *et al.*, 1996a, Dong *et al.*, 2003).

To further evidence the role of gangliosides int HcB entry into m-IC_{cl2} cells, the cells were treated with DL-threo-1-phenyl-2-palmitoyl-amino-3-morpholino-1-propanol (PPMP), an inhibitor of glucosylceramide synthase. HcB-Cy3 internalization in cells exposed to PPMP was significantly lower compared to untreated control cells, whereas subsequent loading with exogenous gangliosides enriched in GD_{1a}, GD_{1b}, and GT_{1b} restored the entry into cells (Fig. 6) further supporting the BoNT/B receptor role of gangliosides.

HcB uptake in intestinal cells does not require synaptotagmin

Syt is a Ca^{++} sensor anchored in synaptic vesicle membrane of neuronal cells, and the isoforms SytI and SytII have been identified as BoNT/B receptors (review in (Rummel, 2013)). SytI and SytII are also expressed in intestinal cells (Sup Fig. 2). Competition experiments were performed by preincubating HcB-Cy3 with a 10 fold excess of SytI or SytII and then incubating the mix with cells for 10 min (Fig. 7). SytII and to a lower extent SytI induced a significant but partial decrease in HcB-Cy3 entry into NG108-15 cells. Indeed, preincubation with SytI or SytII decreased HcB-Cy3 entry into neuronal cells by 30 and 50% (Fig. 7), respectively, in agreement with previous report (Nishiki *et al.*, 1996a). In contrast, no significant inhibitory effect of SytI or SytII was observed in HcB-Cy3 entry into m-IC_{cl2} cells indicating that SytI and SytII are not required for HcB uptake in intestinal cells.

Since the functional BoNT/B receptor on neuronal cells consists of an association of gangliosides and Syt (Nishiki *et al.*, 1994, Nishiki *et al.*, 1996a, Jin *et al.*, 2006, Rummel *et al.*, 2007), we performed competition experiments with combinations of gg and SytI or SytII. A stronger decrease (80%) in HcB-Cy3 internalization into NG108-15 cells was obtained by

This article is protected by copyright. All rights reserved.

preincubation of HcB-Cy3 with gg associated with SytI or SytII (Fig. 8), compared to incubation with SytI or SytII alone, 30 and 50 % inhibition, respectively (Fig. 7). This further confirms that HcB requires both gg and Syt for efficient internalization into neuronal cells. In contrast, preincubation with SytI or SytII did not significantly prevent HcB-Cy3 entry into m-IC_{cl2} cells, and the combination of gg and Syt did not induce additional inhibitory effect compared to gg alone (Fig. 5 and 8) indicating that gangliosides, mainly GD_{1a}/GD_{1b}/GT_{1b}, were sufficient to mediate HcB entry into m-IC_{cl2} cells.

HcB enters neuronal and intestinal cells via a common early endosomal compartment and then follows a distinct non-acidic pathway in intestinal cells

Entry pathways of HcB into m-IC_{cl2} and NG108-15 cells were investigated by colocalization of HcB-Cy3 with markers of specific endosomal compartments. After 10 min incubation at 37°C with both cell types, HcB-Cy3 was distributed in vesicles containing the Rab5 effector EEA1 (early endosome antigen 1) (Fig. 9). Then, endocytosed cargos in early endosomes (EE) can be sorted and transported in distinct intracellular pathways. A major pathway includes the late endosomes (LE)/lysosomes. Rab7 is classically considered as associated with LE/lysosomes. However, Rab5 replacement by Rab7 occurs in EE, and Rab7 seems to have an earlier role in the trafficking between EE and LE/lysosomes (review in (Girard *et al.*, 2014)). As shown in Fig. 10, HcB-Cy3 was found in vesicles containing Rab7 in both m-IC_{cl2} cells and NG108-15 cells after 10 min incubation at 37°C. However, HcB-Cy3 colocalized differently with Lamp1 (lysosomal-associated membrane protein 1) which is a specific marker of LE/lysosomes, in m-IC_{cl2} cells and NG108-15 cells (Fig. 10). In NG108-15 cells, HcB-Cy3 was progressively associated with Lamp1 compartments over time from 5 to 20 min (Fig. 11A, 11C). At 20 min, most of HcB-Cy3 was localized in NG108-15 LE/lysososmes, whereas in m-IC_{cl2} cells only a low level of the fluorescent protein was detected in this intracellular pathway (Fig. 11B, 11C). These results support that the cellular trafficking of HcB differs in neuronal and epithelial intestinal cells.

HcB enters intestinal cells via Cdc42-dependent pathway

RhoGTPases are key regulators which control various cellular functions including diverse endocytosis pathways (Etienne-Manneville *et al.*, 2002). Notably, Cdc42 was found to control a clathrin-independent endocytic process termed the Clathrin-Independent Carrier (CLIC)/GPI-anchored protein-enriched Early Endocytic Compartment (GEEC) pathway and was associated with the endocytosis of GPI-anchored proteins, fluid markers and toxins such

This article is protected by copyright. All rights reserved.

as *Helicobacter pylori* VacA (Sabharanjak *et al.*, 2002, Gauthier *et al.*, 2005, Chadda *et al.*, 2007). Transfection of a Cdc42 negative mutant (Cdc42T17N) fused to GFP into m-IC_{cl2} cells significantly inhibited the entry of HcB-Cy3. None or only a few endocytic vesicles stained with HcB-Cy3 were observed in transfected cells compared to untransfected cells (Fig. 12). In contrast in NG108-15 cells, HcB-Cy3 entry was either unimpaired or only weakly compared to untransfected cells (Fig. 12). Transfection of the dominant negative forms of RhoA (RhoA T17N-GFP) or Rac1 (Rac1 T17N-GFP) in m-IC_{cl2} cells and NG108-15 cells did not significantly prevent HcB-Cy3 entry (Sup. Fig. 3).

DISCUSSION

As monitored with HcB-Cy3, the fluorescent protein bound to the periphery of neuronal cells as well as of intestinal cells and then entered into endocytic vesicles. This raises the question whether BoNT/B recognizes the same specific receptors on both neuronal and intestinal cells? SytI/SytII in combination with gangliosides, mainly GD_{1a}/GD_{1b}/GT_{1b}, were identified as specific BoNT/B receptors on neuronal cells (Nishiki *et al.*, 1994, Nishiki *et al.*, 1996a, Nishiki *et al.*, 1996b, Chai *et al.*, 2006, Jin *et al.*, 2006, Rummel *et al.*, 2007). In addition, SytI/SytII were shown to mediate BoNT/B entry into PC12 cells (Dong *et al.*, 2003). We also confirm that HcB interacts with NG108-15 through gangliosides GD_{1a}/GD_{1b}/GT_{1b} and SytI or SytII by using binding competition experiments (Fig. 4, 5, 6, 7 and 8). The combinations of gangliosides with the receptor protein part (SytI or SytII) were more effective than the individual preparations of gangliosides or Syt in binding inhibition of HcB to NG108-15 cells. This supports that the high affinity functional HcB receptor on neuronal cells requires both the ganglioside and protein parts. In contrast, HcB binding to m-IC_{cl2} cells was fully prevented by gangliosides alone without the help of a protein part such as SytI or SytII. Thereby, SytI or SytII were not involved in HcB receptor on intestinal cells, and gangliosides of the GD_{1a}/GD_{1b}/GT_{1B} series seemed efficient and sufficient receptors for BoNT/B. SytI and SytII are mainly expressed in neuronal cells where they are localized on synaptic vesicle membrane and play a critical role in the evoked release of neurotransmitter (Sudhof, 2013). In addition, SytI has been found to be involved in endocytosis of some compounds such as Na^+-H^+ exchanger in intestinal epithelial cells (Musch *et al.*, 2010). We also observed that intestinal epithelial cells expressed SytI and SytII using Western blot (Sup. Fig. 2). Moreover, SytI and SytII were visualized in m-IC_{cl2} by cell imaging with specific antibodies (Sup. Fig. 2). It is noteworthy that m-IC_{cl2} mainly retains a stem cell profile and can express a wide variety of proteins (Bens *et al.*, 1996). However, SytI and SytII were not

This article is protected by copyright. All rights reserved.

detected by cell imaging in mouse intestinal epithelial cells (Connan *et al.*, 2016), indicating that these proteins are probably weakly expressed in mouse intestinal epithelial cells or only in some cell subpopulations. This further excludes that SytI and SytII have a role in BoNT/B endocytosis in epithelial cells.

The role of gangliosides in HcB entry into intestinal cells was further supported by inhibiting the ganglioside synthesis in m-IC_{cl2} cells with PPMP (Fig. 6). However, this does not preclude the possibility that membrane proteins of intestinal cells might be used in combination with gangliosides for higher BoNT/B affinity receptors. Indeed, BoNT/B did not localize in all cell types of the mouse intestinal epithelium but only in specific cells which represent a preferential passage of the toxin through the intestinal barrier (Connan *et al.*, 2016). In contrast, BoNT/A which uses SV2C as protein receptor on neuronal cells (review in (Rummel, 2013)) enters intestinal cells in a SV2C-dependent manner albeit this molecule has not been evidenced as a BoNT/A receptor in epithelial cells (Elias *et al.*, 2011, Couesnon *et al.*, 2012). This suggests that SV2C might facilitate endocytosis into epithelial cells in a non-specific manner. However, competition assays with SV2C L4 luminal domain and HcB-Cy3 in m-IC_{cL2} cells showed that HcB entry into intestinal cells was not mediated by SV2C (Sup. Fig. 4).

HcB-Cy3 internalization into endocytic vesicles was shown in both neuronal and intestinal cells. However, the distribution of endocytic vesicles containing HcB-Cy3 in both cell types was slightly different. In NG108-15 cells, HcB-Cy3 entered endocytic compartments which migrated in the perinuclear area, whereas in m-IC_{cl2} cells the vesicles containing HcB-Cy3 had a more scattered distribution through the cytoplasm (Fig. 1 and 2). This supports a different trafficking of BoNT/B in intestinal cells versus neuronal cells resulting in a delivery of the whole and active neurotoxin to the basolateral side of intestinal cells. In contrast, in target neuronal cells the neurotoxin is transported in acidic compartments which trigger the translocation of the L chain into the cytosol and its subsequent proteolytic activity towards the SNARE (Soluble N-ethylmaleimide-sensitive-factor Attachment Receptor) synaptobrevin ((Simpson *et al.*, 1994, Keller *et al.*, 2004, Poulain *et al.*, 2008).

HcB-Cy3 uptake was efficiently blocked by Dynasore which is a specific inhibitor of dynamin (Macia *et al.*, 2006) in both neuronal NG108-15 and intestinal m-IC_{cl2} cells (Fig. 3). However, Dynasore not only blocks dynamin-dependent endocytosis but also induces dynamin-independent effects such as reduction of membrane cholesterol, disorganization of lipid rafts, and prevention of actin filament formation involved in membrane ruffling (Preta 2015). Thus, Dynasore could also impair dynamin-independent endocytosis such as

This article is protected by copyright. All rights reserved.

macropinocytosis or fluid phase endocytosis (Preta *et al.*, 2015). The dynamin-dependent entry of HcB-Cy3 into both cell types was further supported by using transfection with the dominant negative dynamin2 K44A (Sup. Fig. 1). A dynamin-based endocytosis has also been evidenced in BoNT/A entry into cells (Couesnon *et al.*, 2009, Harper *et al.*, 2011, Meng *et al.*, 2013). Moreover, K+ depletion experiments indicated that HcB preferentially used a clathrin-independent endocytosis into m-IC_{cl2} cells, contrarily to NG108-15 in which HcB uptake was clathrin-mediated (Fig. 4). Indeed, BoNT/B, like BoNT/A, enters neuronal cells, notably at the neuromuscular junctions, via a clathrin-mediated endocytosis hijacking, at least in part, the synaptic vesicle recycling (Poulain *et al.*, 2008, Meng *et al.*, 2013, Rossetto *et al.*, 2014). Thereby, HcB likely exploited a clathrin-mediated entry into neuronal cells and mainly a clathrin-independent pathway into intestinal cells, both mechanisms of uptake being regulated by dynamin. Interestingly, toxins which recognize glycolipid receptors, use mainly clathrin-independent endocytosis. Toxin binding to membrane glycolipids such as Shiga toxin to globotriaosylceramide or cholera toxin to GM1 induces lipid reorganization (Watkins *et al.*, 2014, Pezeshkian *et al.*, 2016), leading to membrane curvature without clathrin (Romer *et al.*, 2007, Ewers *et al.*, 2010). Membrane invaginations containing toxins are then detached from the plasma membrane through a dynamin-dependent process. This endocytic process is also shared by endogenous proteins such as galectins (Lakshminarayan *et al.*, 2014). BoNT/B possibly uses a similar mechanism of binding to gangliosides GD_{1a}/GD_{1b}/GT_{1b} to trigger a clathrin-independent endocytosis in intestinal epithelial cells.

Cargo molecules attached to membrane receptor are internalized into EE, and then are sorted into multiple endocytic pathways such as recycling to the plasma membrane, transcytosis to the opposite side, or sorted to degradative compartments (LE/lysosomes). Endocytic vesicles are dynamic structures which mature by different ways including fusion with homotypic vesicles or other compartments, or budding and fission in smaller vesicles. Rab proteins are key players in fusion of homotypic endosomes. EEA1 binds to Rab5-GTP and additional effectors such as phosphatidylinositol-3-phosphate (PI3P) and syntaxin-6 in sorting EE where it has a tethering/docking role before membrane fusion. In polarized epithelial cells, EEA1 is distributed in basolateral sorting endosomes but not in apical endosomal compartment suggesting that EEA1 is involved in specific directional endocytic pathway (Simonsen *et al.*, 1998, Christoforidis *et al.*, 1999, Wilson *et al.*, 2000, Shin *et al.*, 2005, Wandinger-Ness *et al.*, 2014). Molecules endocytosed by the typical clathrin-dependent pathway as well as by clathrin-independent pathways are internalized into EE labeled with Rab5 and EEA1 (Kalia *et al.*, 2006, Mayor *et al.*, 2007, Grant *et al.*, 2009,

This article is protected by copyright. All rights reserved.

Howes *et al.*, 2010, Maldonado-Baez *et al.*, 2013). Subsequent maturation of EE into LE is mediated through replacement of Rab5 by Rab7 (Rink *et al.*, 2005, Poteryaev *et al.*, 2010). Thus, Rab7 is found in EE and its activity seems to be required in the late trafficking step from LE to lysosome (Feng *et al.*, 1995), but also in early endosomal sorting in a cargo-dependent manner (Girard *et al.*, 2014). Here, we showed that HcB-Cy3 enters an early endosomal compartment labeled with EEA1 and Rab7 at 10 min incubation in both neuronal and intestinal cells, although HcB was internalized by a clathrin-dependent pathway in NG108-15 cells, and by a clathrin-independent pathway in m-IC_{cl2} cells. Then HcB was transported in distinct intracellular pathways according to the cell type. Overtime from 5 to 20 min, HcB-Cy3 migrated from EE to LE as monitored with Lamp1 in NG108-15 cells, whereas HcB used a distinct pathway in m-IC_{cl2} cells avoiding the passage in LE/lysosomes (Fig. 11 ABC). Therefore, our findings support the hypothesis that the transport in the LE pathway in neuronal cells where the endocytic vesicles are acidified, facilitates the translocation of the L chain into the cytosol and its subsequent inhibitory activity on the neurotransmitter exocytosis machinery. In contrast to neuronal cells, the whole neurotoxin transits through non-acidified vesicles in epithelial cells and is released to the baso-lateral side in an un-dissociated form. Similar findings were observed with BoNT/A (Couesnon *et al.*, 2009).

HcB transport in intestinal cells was further investigated by analyzing the effects of RhoGTPases which are involved in various cellular functions notably in the control of the actin cytoskeleton and also in different endocytic pathways (Hall, 2012). In the epithelial intestinal m-IC_{cl2} cells, HcB-Cy3 was transported in a Cdc42-dependent and Rho- Rac-independent pathway, whereas RhoGTPases were not involved in HcB trafficking in neuronal NG108-15 cells (Fig. 12 and Sup. Fig. 3). Cdc42 is a GTPase of the Rho family which controls certain cortical actin formations like filopodia, cell polarity in all cell types, as well as several intracellular vesicle trafficking and endocytosis pathways including caveolae endocytosis (Tapon *et al.*, 1997, Etienne-Manneville *et al.*, 2002, Cheng *et al.*, 2010, Chi *et al.*, 2013). In addition, Cdc42 controls transcytosis from apical to basolateral side in polarized epithelial cells (Rojas *et al.*, 2001, Harris *et al.*, 2010) such as transcytosis of *Escherichia coli* Shiga-like toxin through intestinal epithelial cells (Malyukova *et al.*, 2009). Moreover, Cdc42 mediates clathrin-independent endocytosis of GPI-anchored proteins, fluid phase markers and toxins in non-neuronal cells such as *H. pylori* VacA, BoNT/A, and cholera toxin subunit B (Sabharanjak *et al.*, 2002, Gauthier *et al.*, 2005, Chadda *et al.*, 2007, Couesnon *et al.*, 2009, Malyukova *et al.*, 2009, Zachos *et al.*, 2014, Chen *et al.*, 2016). The HcB Cdc42-dependent

This article is protected by copyright. All rights reserved.

entry pathway is distinct from that of GEEC (GPI-anchored protein enriched early endosomal compartment) which is associated with GPI-anchored protein uptake and lipid bound ligands, since in contrast to the HcB pathway, GEEC is dynamin-independent and is acidified (Zachos *et al.*, 2014). However, HcB was not transported in the acidified route leading to LE/lysosomes in intestinal cells contrarily to neuronal cells. Cdc42 might regulate several clathrin-independent pathways. Thus in contrast to neuronal cells, HcB similarly to BoNT/A (Couesnon *et al.*, 2010) used a Cdc42-dependent transcytosis in intestinal cells which still remains to be defined.

In conclusion, HcB used distinct entry pathways in neuronal and intestinal cells. HcB recognized gangliosides (GD_{1a}, GD_{1b}, GT_{1B})/synaptotagmins on neuronal cells, whereas gangliosides alone seemed sufficient to facilitate the toxin entry into intestinal cells. In both cell types, HcB uptake was dynamin-dependent, but clathrin-dependent in neuronal cells and clathrin-independent in intestinal cells, and leaded to a common early endosomal compartment labeled with EEA1. Then, HcB was driven into an acidic pathway leading to LE/lysosomes, allowing the translocation of the L chain into the cytosol of neuronal cells, whereas the neurotoxin transcytosed in a Cdc42-dependent manner and released in an un-dissociated form at the basolateral side of epithelial intestinal cells.

EXPERIMENTAL PROCEDURES

Reagents

Endocytosis assay were performed with Dynasore Hydrate (Sigma, 80µM). Competition assay were performed using a mixture of 250 µg ml^{-1} gangliosides (18% GM1, 55% GD_{1a}, 15% GD_{1b}, 10% GT_{1b} and 2% others, Calbiochem) or 50 mg ml^{-1} GM1 (Calbiochem). PPMP was from Sigma. Cells were stained with Hoechst 33342 (Invitrogen, 1:1000 dilution) for the nuclei. The primary antibodies used recognized E- cadherin (Invitrogen, rat, 1:250 dilution), EEA1 (BD Pharmingen^{TM,} mouse IgG1, 1:400 dilution), Rab7 (Cell Signaling, Rabbit, 1:200 dilution), and and Lamp1 (BD Pharmingen^{TM}, rat, 1:500). The secondary antibodies were Alexa fluor 488 goat anti rat, (Invitrogen, 1:500 dilution). Rat synaptotagmin I (amino acids 1-421) and II (amino acids 8-61) were produced as recombinant proteins with N-terminal 6His-tag from pET28 vector. Rabbit anti-SytI (ab68853) and SytII (ab113545) were from Abcam, mouse monoclonal antibodies against SytI (3F10A) and SytII (8G2b) were provided by C. Leveque (Nishiki *et al.*, 1996a, Charvin *et al.*, 1997).

This article is protected by copyright. All rights reserved.

Recombinant HcB

Recombinant His-tag Hc fragment of BoNT/B was produced and purified from pET28a vector containing DNA encoding for HcB cloned into *BamHI* and *SalI* sites, as previously described (Tavallaie *et al.*, 2004). HcB His-tag was labeled with Amersham Cy3 Mono-Reactive Dye Pack (GE Healthcare) according to the manufacturer's recommendations. Free dye was removed from labeled protein using the de Zeba Spin Desalting columns according to the manufacturer's recommendations (Thermo Scientific).

Cell cultures

NG108-15 neuronal cells were obtained from the ATCC, and m-IC_{cl2} cells were kindly provided by A. Vandewalle (URMS 1149, Paris). Cells were cultured at 37°C in a 5% CO_2 atmosphere and medium was changed every second day. NG108-15 cells were maintained in Dulbecco's modified Eagle's medium (DMEM, Invitrogen) supplemented with 10% fetal calf serum (FCS, Invitrogen). m-IC_{cl2} cells were cultured as described previously (Bens *et al.*, 1996).

For m-IC_{cl2} cells grown on filters, cells were seeded (1 x 105) on the upper chamber of Transwell Inserts (Corning) and allowed to differentiate for one week. Cells were incubated with HcB-Cy3 (2.5 μg/ml) for 3 min at 37°C and were rinsed three times with culture medium containing BSA 0.1% and were further incubated at 37°C for the indicated times. Cells were washed with cold PBS and fixed with 4% paraformaldehyde (PFA) before phalloidin labeling.

Primary cortical neurons were obtained from fetal mice. Cortices from E17 mouse embryos were dissected, cut into small pieces, and treated with 0.3% protease for 10 min before trituration in PBS–0.1% DNAse (Roche). Dissociated cells were centrifuged through 4% bovine serum albumin (BSA) solution for 4 min at 1000 rpm. Cells were resuspended in Neurobasal medium supplemented with 2% fetal calf serum, 2%B27 supplement, 25M -mercaptoethanol, 2 mM glutamine, and 50g/mL gentamicin. Cells were plated at a density of 5x 104cells/cm2 on round coverslips or glass-bottomed microwell dishes (MatTek, Ashland, US) previously coated with 50 μg/mL poly-ornithine followed by 5 μg/mL laminine. After 1 day, cells were treated with 25 μg/mL uridine and 10 μg/mL fluorode-oxyuridine to eliminate proliferating glial cells (Chen *et al.*, 2006).

Binding and internalization studies

This article is protected by copyright. All rights reserved.

Accepted Article

Cells (5 X 10^4) were plated on coverslips and incubated in HBSS/BSA 0.5% (HBSS/BSA) containing 5 µg/ml of HcB-Cy3. For internalization experiments, cells were incubated at 37°C for 3 min, washed with HBSS, and either fixed with 4% PFA in PBS for 20 min, or further incubated at 37°C in HBSS before fixation. After washing in PBS and quenching with 50mM NH_4Cl in PBS, cells were permeabilized with 0.2% Triton X-100 in PBS and incubated with Alexa647-labeled phalloidin (Interchim) and Dapi.

For competition studies, cells plated on coverslips (5 x 10^4) were incubated with HcB-Cy3 (2.5 µg) for 10 minutes or HcB-Cy3 (2.5 µg) pre-incubated with gangliosides mix (250 µg ml^{-1}), or Syt I (25 µg) or Syt II (25 µg) or a combination of gangliosides mix and Syt I or Syt II for 30 minutes at room temperature.

Ganglioside depletion in cell membrane with PPMP was performed as previously described (Couesnon *et al.*, 2008) by incubating m-IC_{cl2} cells with 7.5 µg/ml PPMP in culture medium for 48 h. Ganglioside complementation was performed by incubating the cells with the ganglioside mixture (250 µg/ml) in culture medium after 24 h of PPMP treatment.

K+ depletion was performed as previously described (Couesnon *et al.*, 2010). Briefly, cells were incubated in K+ depletion buffer (NaCl 140 mM, $CaCl_2$ 1 mM, $MgCl_2$ 1 mM, Hepes 20 mM, D-glucose 1 gl^{-1}, pH 7.4) for 30 min at 37°C followed by hypotonic shock (potassium depletion buffer diluted 1:2 in distillated water) for 5 min at 37°C. Control cells were incubated in HBSS containing 10 mM KCl. Cells were then incubated with HcB-Cy3 for 10 min at 37°C and processed for microscopy.

Cell transfections

Eukaryotic plasmid vectors used in this work are as follows: GFP-Cdc42T17 N (C. Lamaze, Institut Curie, Paris, France). Cell transfections were performed using X-tremeGene HP (Roche) according to the manufacturer's instructions. Briefly, cells were grown over night on coverslip. DNA- lipid complexes were formed for 10 minutes at 37°C and added dropwise to the cells and further incubated for 4 h at 37°C. The cells were then washed in PBS and grown overnight to allow expression of proteins from plasmid-borne gene. Cells were then incubated for 10 minutes with HcB-Cy3 before PFA fixation.

ACKNOWLEDGEMENTS

We thank C. Leveque for the rat synaptotagmin I and II vectors.

This article is protected by copyright. All rights reserved.

REFERENCES

Tetanus surveillance --- United States, 2001-2008. *MMWR Morb Mortal Wkly Rep* **60,** 365-369.

Ahsan, C.R., Hajnoczky, G., Maksymowych, A.B. and Simpson, L.L. (2005). Visualization of binding and transcytosis of botulinum toxin by human intestinal epithelial cells. *J. Pharmacol. Exp. Ther.* **315,** 1028-1035.

Arnon, S.S. (1989) Infant botulism. In *Anaerobic infections in humans*, S.M. Finegold, W.L. George (eds.). San Diego, CA, Academic Press, pp. 601-609.

Barash, J.R. and Arnon, S.S. (2014). A Novel Strain of *Clostridium botulinum* That Produces Type B and Type H Botulinum Toxins. *J Infect Dis.* **209,** 183-191. doi: 110.1093/infdis/jit1449. Epub 2013 Oct 1097.

Beard, M. (2014) Translocation, entry into the cell. In *Molecular Aspects of Botulinum Neurotoxins*, K.A. Foster (ed.). Springer, pp. 151-170.

Bens, M., Bogdanova, A., Cluzeaud, F., Miquerol, L., Kerneis, S., Kraehenbuhl, J.P*., et al.* (1996). Transimmortalized mouse intestinal cells (m-ICc12) that maintain a crypt phenotype. *Am J Physiol* **270,** C1666-1674.

Bohnert, S. and Schiavo, G. (2005). Tetanus toxin is transported in a novel neuronal compartment characterized by a specialized pH regulation. *J. Biol. Chem.* **280,** 42336-42344.

Brashear, A., Lew, M.F., Dykstra, D.D., Comella, C.L., Factor, S.A., Rodnitzky, R.L*., et al.* (1999). Safety and efficacy of NeuroBloc (botulinum toxin type B) in type A-responsive cervical dystonia. *Neurology* **53,** 1439-1446.

Brook, I. (2007). Infant botulism. *J Perinatol* **27,** 175-180.

Carpentier, J.L., Sawano, F., Geiger, D., Gorden, P., Perrelet, A. and Orci, L. (1989). Potassium depletion and hypertonic medium reduce "non-coated" and clathrin-coated pit formation as well as endocytosis through these two gates. *J. Cell Physiol.* **138,** 519-526.

Chadda, R., Howes, M.T., Plowman, S.J., Hancock, J.F., Parton, R.G. and Mayor, S. (2007). Cholesterol-sensitive Cdc42 activation regulates actin polymerization for endocytosis via the GEEC pathway. *Traffic* **8,** 702-717.

Chai, Q., Arndt, J.W., Dong, M., Tepp, W.H., Johnson, E.A., Chapman, E.R. and Stevens, R.C. (2006). Structural basis of cell surface receptor recognition by botulinum neurotoxin B. *Nature* **444,** 1096-1100.

Charvin, N., L'Eveque, C., Walker, D., Berton, F., Raymond, C., Kataoka, M*., et al.* (1997). Direct interaction of the calcium sensor protein synaptotagmin I with a cytoplasmic domain of the alpha1A subunit of the P/Q-type calcium channel. *EMBO J* **16,** 4591-4596.

Chen, F., Vitry, S., Hocquemiller, M., Desmaris, N., Ausseil, J. and Heard, J.M. (2006). alpha-L-Iduronidase transport in neurites. *Mol Genet Metab* **87,** 349-358.

Chen, H., Gao, Z., He, C., Xiang, R., van Kuppevelt, T.H., Belting, M. and Zhang, S. (2016). GRP75 upregulates clathrin-independent endocytosis through actin cytoskeleton reorganization mediated by the concurrent activation of Cdc42 and RhoA. *Exp Cell Res* **343,** 223-236.

Cheng, Z.J., Singh, R.D., Holicky, E.L., Wheatley, C.L., Marks, D.L. and Pagano, R.E. (2010). Co-regulation of caveolar and Cdc42-dependent fluid phase endocytosis by phosphocaveolin-1. *J Biol Chem* **285,** 15119-15125.

Cherington, M. (1998). Clinical spectrum of botulism. *Muscle Nerve* **21,** 701-710.

Chi, X., Wang, S., Huang, Y., Stamnes, M. and Chen, J.L. (2013). Roles of rho GTPases in intracellular transport and cellular transformation. *Int J Mol Sci* **14,** 7089-7108.

This article is protected by copyright. All rights reserved.

Christoforidis, S., McBride, H.M., Burgoyne, R.D. and Zerial, M. (1999). The Rab5 effector EEA1 is a core component of endosome docking. *Nature* **397,** 621-625.

Connan, C., Varela-Chavez, C., Mazuet, C., Molgo, J., Haustant, G.M., Disson, O.*, et al.* (2016). Translocation and dissemination to target neurons of botulinum neurotoxin type B in the mouse intestinal wall. *Cell Microbiol* **18,** 282-301.

Couesnon, A., Colasante, C., Molgo, J. and Popoff, M.R. (2010). Differential entry of Botulinum neurotoxin A into neuronal and intestinal cells: an ultrastructural approach. *Botulinum J.* **1,** 375-392.

Couesnon, A., Molgo, J., Connan, C. and Popoff, M.R. (2012). Preferential entry of botulinum neurotoxin A Hc domain trhough intestinal crypt cells and targeting to cholinergic neurons of the mouse intestine. *PLoS Pathog* **8,** e1002583.

Couesnon, A., Pereira, Y. and Popoff, M.R. (2008). Receptor-mediated transcytosis of botulinum neurotoxin A through intestinal cell monolayers. *Cell. Microbiol.* **10,** 375-387.

Couesnon, A., Shimizu, T. and Popoff, M.R. (2009). Differential entry of botulinum neurotoxin A into neuronal and intestinal cells. *Cell Microbiol* **11,** 289-308.

Dong, M., Richards, D.A., Goodnough, M.C., Tepp, W.H., Johnson, E.A. and Chapman, E.R. (2003). Synaptotagmins I and II mediate entry of botulinum neurotoxin B into cells. *J. Cell Biol.* **162,** 1293-1303.

Elias, M., Al-Saleem, F., Ancharski, D.M., Singh, A., Nasser, Z., Olson, R.M. and Simpson, L.L. (2011). Evidence that botulinum toxin receptors on epithelial cells and neuronal cells are not identical: implications for development of a non-neurotropic vaccine. *J Pharmacol Exp Ther* **336,** 605-612.

Etienne-Manneville, S. and Hall, A. (2002). Rho GTPases in cell biology. *Nature* **420,** 629-635.

Ewers, H., Romer, W., Smith, A.E., Bacia, K., Dmitrieff, S., Chai, W.*, et al.* (2010). GM1 structure determines SV40-induced membrane invagination and infection. *Nat Cell Biol* **12,** 11-18; sup pp 11-12.

Feng, Y., Press, B. and Wandinger-Ness, A. (1995). Rab 7: an important regulator of late endocytic membrane traffic. *J Cell Biol* **131,** 1435-1452.

Fenicia, L. and Anniballi, F. (2009). Infant botulism. *Ann Ist Super Sanita* **45,** 134-146.

Fox, C.K., Keet, C.A. and Strober, J.B. (2005). Recent advances in infant botulism. *Pediatr Neurol* **32,** 149-154.

Fujinaga, Y., Inoue, K., Watanabe, S., Yokota, K., Hirai, Y., Nagamachi, E. and Oguma, K. (1997). The haemagglutinin of *Clostridium botulinum* type C progenitor toxin plays an essential role in binding of toxin to the epithelial cells of guinea pig intestine, leading to the efficient absorption of the toxin. *Microbiol.* **143,** 3841-3847.

Gauthier, N.C., Monzo, P., Kaddai, V., Doye, A., Ricci, V. and Boquet, P. (2005). *Helicobacter pylro* VacA cytotoxin: a probe for a clathrin-independent and Cdc42-dependent pinocytic pathway routed to late endosomes. *Mol Biol Cell* **16,** 4852-4866.

Girard, E., Chmiest, D., Fournier, N., Johannes, L., Paul, J.L., Vedie, B. and Lamaze, C. (2014). Rab7 is functionally required for selective cargo sorting at the early endosome. *Traffic* **15,** 309-326.

Grant, B.D. and Donaldson, J.G. (2009). Pathways and mechanisms of endocytic recycling. *Nat Rev Mol Cell Biol* **10,** 597-608.

Gu, S., Rumpel, S., Zhou, J., Strotmeier, J., Bigalke, H., Perry, K.*, et al.* (2012). Botulinum neurotoxin is shielded by NTNHA in an interlocked complex. *Science* **335,** 977-981.

Hall, A. (2012). Rho family GTPases. *Biochem Soc Trans.* **40,** 1378-1382. doi: 1310.1042/BST20120103.

This article is protected by copyright. All rights reserved.

Harper, C.B., Martin, S., Nguyen, T.H., Daniels, S.J., Lavidis, N.A., Popoff, M.R., *et al.* (2011). Dynamin inhibition blocks botulinum neurotoxin type A endocytosis in neurons and delays botulism. *J. Biol. Chem.* **286,** 35966-35976.

Harris, K.P. and Tepass, U. (2010). Cdc42 and vesicle trafficking in polarized cells. *Traffic* **11,** 1272-1279.

Hill, K.K. and Smith, T.J. (2013). Genetic diversity within *Clostridium botulinum* serotypes, botulinum neurotoxin gene clusters and toxin subtypes. *Curr Top Microbiol Immunol* **364,** 1-20.

Howes, M.T., Mayor, S. and Parton, R.G. (2010). Molecules, mechanisms, and cellular roles of clathrin-independent endocytosis. *Curr Opin Cell Biol* **22,** 519-527.

Hughes, J.M., Blumenthal, J.R., Merson, M.H., Lombard, G.L., Dowell, V.R., Jr. and Gangarosa, E.J. (1981). Clinical features of types A and B food-borne botulism. *Ann Intern Med* **95,** 442-445.

Inui, K., Sagane, Y., Miyata, K., Miyashita, S., Suzuki, T., Shikamori, Y., *et al.* (2012). Toxic and nontoxic components of botulinum neurotoxin complex are evolved from a common ancestral zinc protein. *Biochem Biophys Res Commun* **419,** 500-504.

Jin, R., Rummel, A., Binz, T. and Brunger, A.T. (2006). Botulinum neurotoxin B recognizes its protein receptor with high affinity and specificity. *Nature* **444,** 1092-1095.

Jin, Y., Takegahara, Y., Sugawara, Y., Matsumura, T. and Fujinaga, Y. (2009). Disruption of the epithelial barrier by botulinum haemagglutinin (HA) proteins - differences in cell tropism and the mechanism of action between HA proteins of types A or B, and HA proteins of type C. *Microbiology* **155,** 35-45.

Kalia, M., Kumari, S., Chadda, R., Hill, M.M., Parton, R.G. and Mayor, S. (2006). Arf6-independent GPI-anchored protein-enriched early endosomal compartments fuse with sorting endosomes via a Rab5/phosphatidylinositol-3'-kinase-dependent machinery. *Mol Biol Cell* **17,** 3689-3704.

Keller, J.E., Cai, F. and Neale, E.A. (2004). Uptake of botulinum neurotoxin into cultured neurons. *Biochem.* **43,** 526-532.

Kovbasnjuk, O., Edidin, M. and Donowitz, M. (2001). Role of lipid rafts in Shiga toxin 1 interaction with the apical surface of Caco-2 cells. *J Cell Sci* **114,** 4025-4031.

Lakshminarayan, R., Wunder, C., Becken, U., Howes, M.T., Benzing, C., Arumugam, S., *et al.* (2014). Galectin-3 drives glycosphingolipid-dependent biogenesis of clathrin-independent carriers. *Nat Cell Biol* **16,** 595-606.

Lalli, G., Gschmeissner, S. and Schiavo, G. (2003). Myosin Va and microtubule-based motors are required for fast axonal retrograde transport of tetanus toxin in motor neurons. *J Cell Sci* **116,** 4639-4650.

Lam, T.I., Stanker, L.H., Lee, K., Jin, R. and Cheng, L.W. (2015). Translocation of botulinum neurotoxin serotype A and associated proteins across the intestinal epithelia. *Cell Microbiol* **17,** 1133-1143.

Lee, K., Zhong, X., Gu, S., Kruel, A.M., Dorner, M.B., Perry, K., *et al.* (2014). Molecular basis for disruption of E-cadherin adhesion by botulinum neurotoxin A complex. *Science.* **344,** 1405-1410. doi: 1410.1126/science.1253823.

Macia, E., Ehrlich, M., Massol, R., Boucrot, E., Brunner, C. and Kirchhausen, T. (2006). Dynasore, a cell-permeable inhibitor of dynamin. *Dev Cell.* **10,** 839-850.

Maksymowych, A.B. and Simpson, L.I. (2004). Structural features of the botulinum neurotoxin molecule that govern binding and transcytosis across polarized human intestinal epithelial cells. *J. Pharmacol. Exp. Ther.* **310,** 633-641.

Maksymowych, A.B. and Simpson, L.L. (1998). Binding and transcytosis of botulinum neurotoxin by polarized human carcinoma cells. *J. Biol. Chem.* **273,** 21950-21957.

This article is protected by copyright. All rights reserved.

Maldonado-Baez, L., Williamson, C. and Donaldson, J.G. (2013). Clathrin-independent endocytosis: a cargo-centric view. *Exp Cell Res* **319,** 2759-2769.

Malyukova, I., Murray, K.F., Zhu, C., Boedeker, E., Kane, A., Patterson, K.*, et al.* (2009). Macropinocytosis in Shiga toxin 1 uptake by human intestinal epithelial cells and transcellular transcytosis. *Am J Physiol Gastrointest Liver Physiol* **296,** G78-92.

Maslanka, S.E., Luquez, C., Dykes, J.K., Tepp, W.H., Pier, C.L., Pellett, S.*, et al.* (2016). A Novel Botulinum Neurotoxin, Previously Reported as Serotype H, Has a Hybrid-Like Structure With Regions of Similarity to the Structures of Serotypes A and F and Is Neutralized With Serotype A Antitoxin. *J Infect Dis* **213,** 379-385.

Mayor, S. and Pagano, R.E. (2007). Pathways of clathrin-independent endocytosis. *Nat Rev Mol Cell Biol* **8,** 603-612.

Meng, J., Wang, J., Lawrence, G.W. and Dolly, J.O. (2013). Molecular components required for resting and stimulated endocytosis of botulinum neurotoxins by glutamatergic and peptidergic neurons. *FASEB J.* **27,** 3167-3180. doi: 3110.1096/fj.3113-228973. Epub 222013 May 228972.

Merz, B., Bigalke, H., Stoll, G. and Naumann, M. (2003). Botulism type B presenting as pure autonomic dysfunction. *Clin Auton Res* **13,** 337-338.

Musch, M.W., Arvans, D.L., Wang, Y., Nakagawa, Y., Solomaha, E. and Chang, E.B. (2010). Cyclic AMP-mediated endocytosis of intestinal epithelial NHE3 requires binding to synaptotagmin 1. *Am J Physiol Gastrointest Liver Physiol* **298,** G203-211.

Nishikawa, A., Uotsu, N., Arimitsu, H., Lee, J.C., Miura, Y., Fujinaga, Y.*, et al.* (2004). The receptor and transporter for internalization of *Clostridium botulinum* type C progenitor toxin into HT-29 cells. *Biochem. Biophys. Res. Commun.* **319,** 327-333.

Nishiki, T., Kamata, Y., Nemoto, Y., Omori, A., Ito, T., Takahashi, M. and Kozaki, S. (1994). Identification of protein receptor for *Clostridium botulinum* type B neurotoxin in rat brain synaptosomes. *J. Biol. Chem.* **269,** 10498-10503.

Nishiki, T., Tokuyama, Y., Kamata, Y., Nemoto, Y., Yoshida, A., Sato, K.*, et al.* (1996a). The high-affinity of *Clostridium botulinum* type B neurotoxin to synaptotagmin II associated with gangliosides G_{T1B}/G_{D1a}. *FEBS Lett.* **378,** 253-257.

Nishiki, T., Tokuyama, Y., Kamata, Y., Nemoto, Y., Yoshida, A., Sekiguchi, M.*, et al.* (1996b). Binding of botulinum type B neurotoxin to Chinese hamster ovary cells transfected with rat synaptotagmin II cDNA. *Neurosci Lett* **208,** 105-108.

Oguma, K., Inoue, K., Fujinaga, Y., Yokota, K., Watanabe, T., Ohyama, T.*, et al.* (1999). Structure and function of *Clostridium botulinum* progenitor toxin. *J. Toxicol.* **18,** 17-34.

Park, J.B. and Simpson, L.L. (2003). Inhalation poisoning by botulinum toxin and inhalation vaccination with its heavy-chain component. *Infect. Immun.* **71,** 1147-1154.

Peck, M.W., Smith, T.J., Anniballi, F., Austin, J.W., Bano, L., Bradshaw, M.*, et al.* (2017). Historical Perspectives and Guidelines for Botulinum Neurotoxin Subtype Nomenclature. *Toxins (Basel)* **9**.

Pezeshkian, W., Hansen, A.G., Johannes, L., Khandelia, H., Shillcock, J.C., Kumar, P.B. and Ipsen, J.H. (2016). Membrane invagination induced by Shiga toxin B-subunit: from molecular structure to tube formation. *Soft Matter* **12,** 5164-5171.

Popoff, M.R. and Marvaud, J.C. (1999) Structural and genomic features of clostridial neurotoxins. In *The Comprehensive Sourcebook of Bacterial Protein Toxins*, J.E. Alouf, J.H. Freer (eds.) 2 edn. London, Academic Press, pp. 174-201.

Popoff, M.R., Mazuet, C. and Poulain, B. (2013) Botulism and Tetanus. In *The Prokaryotes: Human Microbiology*, 4° edn. Berlin Heidelberg, Springer-Verlag, pp. 247-290.

Poteryaev, D., Datta, S., Ackema, K., Zerial, M. and Spang, A. (2010). Identification of the switch in early-to-late endosome transition. *Cell* **141,** 497-508.

This article is protected by copyright. All rights reserved.

Potulska-Chromik, A., Zakrzewska-Pniewska, B., Szmidt-Salkowska, E., Lewandowski, J., Sinski, M., Przyjalkowski, W. and Kostera-Pruszczyk, A. (2013). Long lasting dysautonomia due to botulinum toxin B poisoning: clinical-laboratory follow up and difficulties in initial diagnosis. *BMC Res Notes.* **6:438.,** 10.1186/1756-0500-1186-1438.

Poulain, B., Popoff, M.R. and Molgo, J. (2008). How do the botulinum neurotoxins block neurotransmitter release: from botulism to the molecular mechanism of action. *Botulinum J.* **1,** 14-87.

Preta, G., Cronin, J.G. and Sheldon, I.M. (2015). Dynasore - not just a dynamin inhibitor. *Cell Commun Signal* **13,** 24.

Quinn, C.P. and Minton, N.P. (2001) Clostridial neurotoxins. In *Clostridia*, H. Bahl, P. Dürre (eds.). Veinheim, Willey-VCH, pp. 211-250.

Restani, L., Giribaldi, F., Manich, M., Bercsenyi, K., Menendez, G., Rossetto, O.*, et al.* (2012). Botulinum neurotoxins A and E undergo retrograde axonal transport in primary motor neurons. *PLoS Pathog* **8,** e1003087.

Rink, J., Ghigo, E., Kalaidzidis, Y. and Zerial, M. (2005). Rab conversion as a mechanism of progression from early to late endosomes. *Cell* **122,** 735-749.

Rojas, R., Ruiz, W.G., Leung, S.M., Jou, T.S. and Apodaca, G. (2001). Cdc42-dependent modulation of tight junctions and membrane protein traffic in polarized Madin-Darby canine kidney cells. *Mol. Biol. Cell* **12,** 2257-2274.

Romer, W., Berland, L., Chambon, V., Gaus, K., Windschiegl, B., Tenza, D.*, et al.* (2007). Shiga toxin induces tubular membrane invaginations for its uptake into cells. *Nature* **450,** 670-675.

Rosow, L.K. and Strober, J.B. (2015). Infant botulism: review and clinical update. *Pediatr Neurol* **52,** 487-492.

Rossetto, O., Pirazzini, M. and Montecucco, C. (2014). Botulinum neurotoxins: genetic, structural and mechanistic insights. *Nat Rev Microbiol.* **12,** 535-549. doi: 510.1038/nrmicro3295. Epub 2014 Jun 1030.

Roux, S., Saint Cloment, C., Curie, T., Girard, E., Mena, F.J., Barbier, J.*, et al.* (2006). Brain-derived neurotrophic factor facilitates in vivo internalization of tetanus neurotoxin C-terminal fragment fusion proteins in mature mouse motor nerve terminals. *Eur J Neurosci* **24,** 1546-1554.

Rummel, A. (2013). Double receptor anchorage of botulinum neurotoxins accounts for their exquisite neurospecificity. *Curr Top Microbiol Immunol* **364:61-90.,** 10.1007/1978-1003-1642-33570-33579_33574.

Rummel, A., Eichner, T., Weil, T., Karnath, T., Gutcaits, A., Mahrhold, S.*, et al.* (2007). Identification of the protein receptor binding site of botulinum neurotoxins B and G proves the double-receptor concept. *Proc Natl Acad Sci U S A* **104,** 359-364.

Sabharanjak, S., Sharma, P., Parton, R.G. and Mayor, S. (2002). GPI-anchored proteins are delivered to recycling endosomes via a distinct cdc42-regulated, clathrin-independent pinocytic pathway. *Develop. Cell* **2,** 411-423.

Sagane, Y., Miyashita, S., Miyata, K., Matsumoto, T., Inui, K., Hayashi, S.*, et al.* (2012). Small-angle X-ray scattering reveals structural dynamics of the botulinum neurotoxin associating protein, nontoxic nonhemagglutinin. *Biochem Biophys Res Commun* **425,** 256-260.

Sharma, S.K., Ramzan, M.A. and Singh, B.R. (2003). Separation of the components of type A botulinum neeurotoxin complex by electrophoresis. *Toxicon* **41,** 321-331.

Shin, H.W., Hayashi, M., Christoforidis, S., Lacas-Gervais, S., Hoepfner, S., Wenk, M.R.*, et al.* (2005). An enzymatic cascade of Rab5 effectors regulates phosphoinositide turnover in the endocytic pathway. *J Cell Biol* **170,** 607-618.

This article is protected by copyright. All rights reserved.

Simonsen, A., Lippe, R., Christoforidis, S., Gaullier, J.M., Brech, A., Callaghan, J., *et al.* (1998). EEA1 links PI(3)K function to Rab5 regulation of endosome fusion. *Nature* **394,** 494-498.

Simpson, L.L., Coffield, J.A. and Bakry, N. (1994). Inhibition of vacuolar adenosine triphosphatase antagonizes the effects of clostridial neurotoxins but not phospholipase A2 neurotoxins. *J. Pharmacol. Exp. Ther.* **269,** 256-262.

Sobel, J. (2005). Botulism. *Clin Infect Dis* **41,** 1167-1173.

Sudhof, T.C. (2013). Neurotransmitter release: the last millisecond in the life of a synaptic vesicle. *Neuron* **80,** 675-690.

Sugawara, Y. and Fujinaga, Y. (2011). The botulinum toxin complex meets E-cadherin on the way to its destination. *Cell Adh Migr* **5,** 34-36.

Sugawara, Y., Matsumura, T., Takegahara, Y., Jin, Y., Tsukasaki, Y., Takeichi, M. and Fujinaga, Y. (2010). Botulinum hemagglutinin disrupts the intercellular epithelial barrier by directly binding E-cadherin. *J Cell Biol* **189,** 691-700.

Tapon, N. and Hall, A. (1997). Rho, Rac and CDC42 GTPases regulate the organization of the actin cytoskeleton. *Cur. Biol.* **9,** 86-92.

Tavallaie, M., Chenal, A., Gillet, D., Pereira, Y., Manich, M., Gibert, M., *et al.* (2004). Interaction between the two subdomains of the C-terminal part of the botulinum neurotoxin A is essential for the generation of protective antibodies. *FEBS Lett.* **572,** 299-306.

Wandinger-Ness, A. and Zerial, M. (2014). Rab proteins and the compartmentalization of the endosomal system. *Cold Spring Harb Perspect Biol* **6,** a022616.

Watkins, E.B., Gao, H., Dennison, A.J., Chopin, N., Struth, B., Arnold, T., *et al.* (2014). Carbohydrate conformation and lipid condensation in monolayers containing glycosphingolipid Gb3: influence of acyl chain structure. *Biophys J* **107,** 1146-1155.

Wilson, J.M., de Hoop, M., Zorzi, N., Toh, B.H., Dotti, C.G. and Parton, R.G. (2000). EEA1, a tethering protein of the early sorting endosome, shows a polarized distribution in hippocampal neurons, epithelial cells, and fibroblasts. *Mol Biol Cell* **11,** 2657-2671.

Woodruff, B.A., Griffin, P.M., McCroskey, L.M., Smart, J.F., Wainwright, R.B., Bryant, R.G., *et al.* (1992). Clinical and laboratory comparison of botulism from toxin types A, B, and E in the United States, 1975-1988. *J Infect Dis* **166,** 1281-1286.

Zachos, N.C., Alamelumangpuram, B., Lee, L.J., Wang, P. and Kovbasnjuk, O. (2014). Carbachol-mediated endocytosis of NHE3 involves a clathrin-independent mechanism requiring lipid rafts and Cdc42. *Cell Physiol Biochem* **33,** 869-881.

Accepted Article

This article is protected by copyright. All rights reserved.

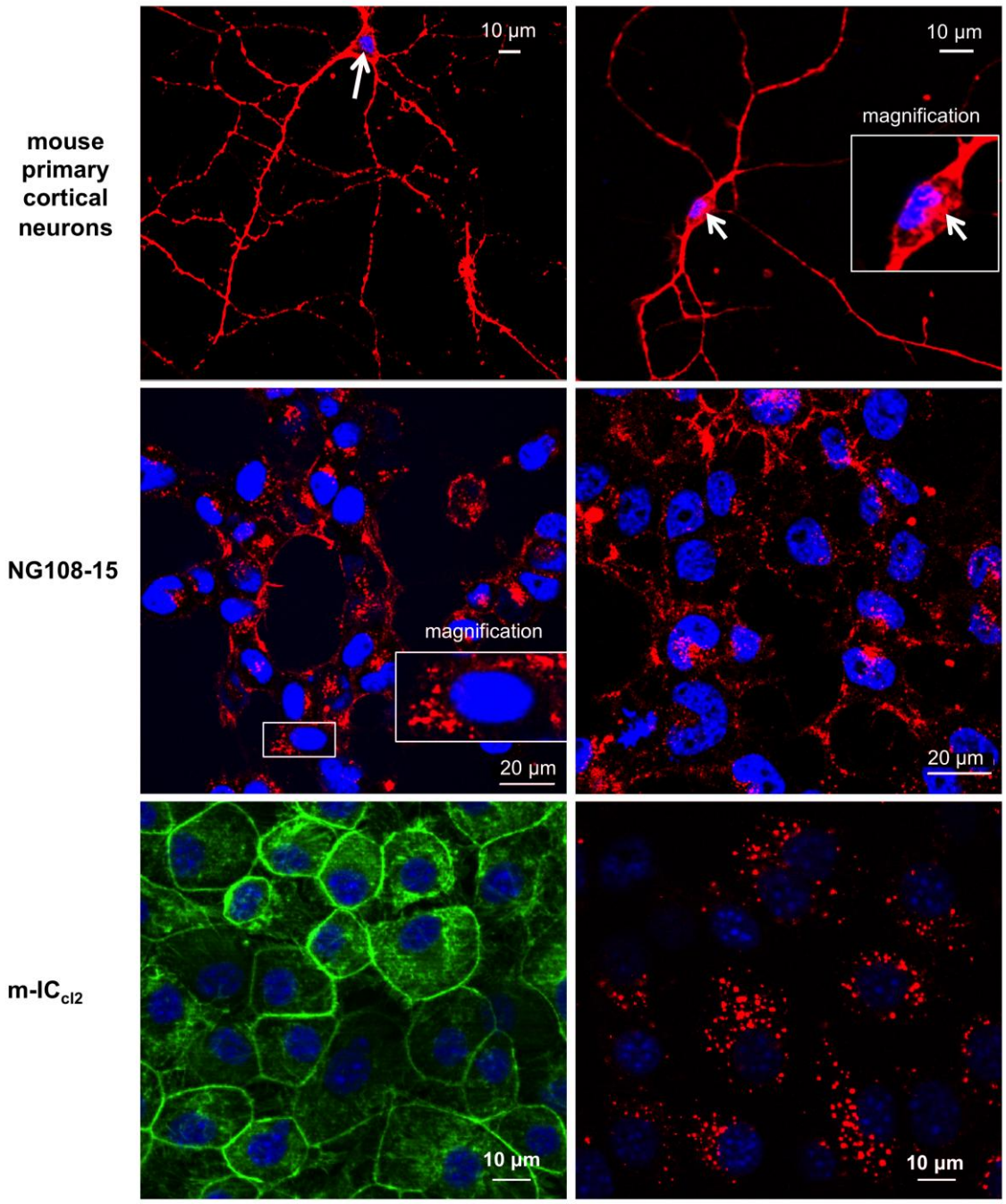


Figure 1. HcB-Cy3 entry into neuronal primary cells, NG108-15 and intestinal crypt m-IC$_{cl2}$ cells.

Mouse primary cortical neurons, NG108-15, or m-IC$_{cl2}$ cells plated on glass slides were incubated with HcB-Cy3 (2.5 µg/ml) for 10 min at 37°C. Then, the cells were fixed and mounted for microscopy observation. Cells were counterstained with Dapi to visualize nuclei, and m-IC$_{cl2}$ cells were counterstained with phalloidin (green) to visualize the actin cytoskeleton.

This article is protected by copyright. All rights reserved.

White arrows indicate neuronal cell bodies with internalized HcB-Cy3 in intracellular compartments. InternalizedHcB-Cy3 appeared as numerous vesicular spots in m-IC_{cl2} cells.

Accepted Article

This article is protected by copyright. All rights reserved.

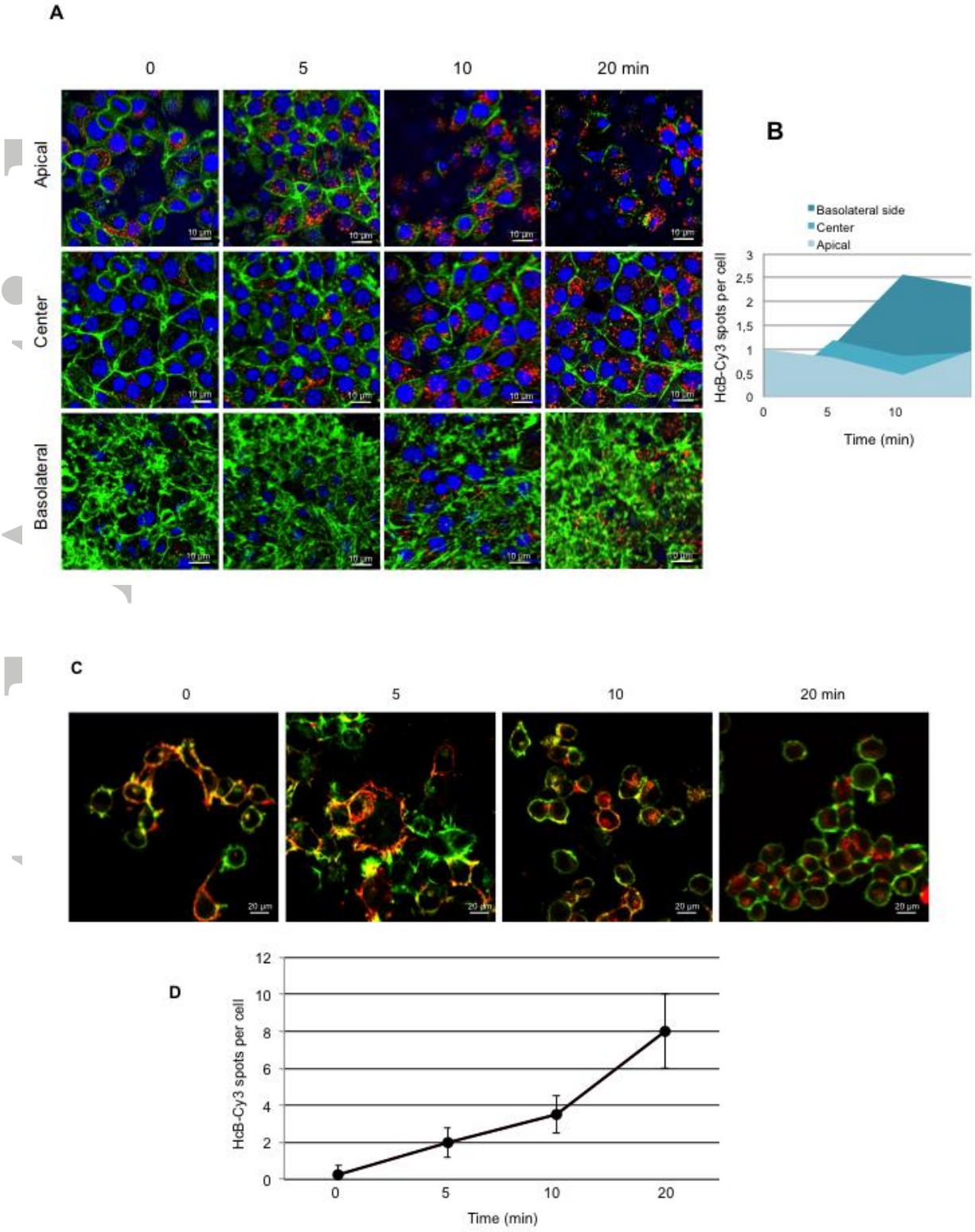


Figure 2. HcB-Cy3 passage through polarized intestinal crypt m-IC$_{cl2}$ cells.

(A) HcB-Cy3 (2.5 µg/ml) was added to the apical chamber of polarized m-IC$_{cl2}$ cells grown on filters for 3 min at 37°C. Then, the culture medium was replaced with Dulbecco's medium. The cells were further incubated at 37°C for the indicated times, fixed and processed for confocal microscopy.

This article is protected by copyright. All rights reserved.

(B and D) Intracellular HcB-Cy3 was quantified and expressed as the number of HcB-Cy3 spots in apical, center, or basolateral side per cell. Values are means from three independent experiments with three replicates each.

(C) HcB-Cy3 (2.5 μg/ml) was added to NG108-15 grown on cover slides for 3 min at 37°C. Then, the culture medium was replaced with Dulbecco's medium. The cells were further incubated at 37°C for the indicated times, fixed and processed for confocal microscopy.

Accepted Article

This article is protected by copyright. All rights reserved.

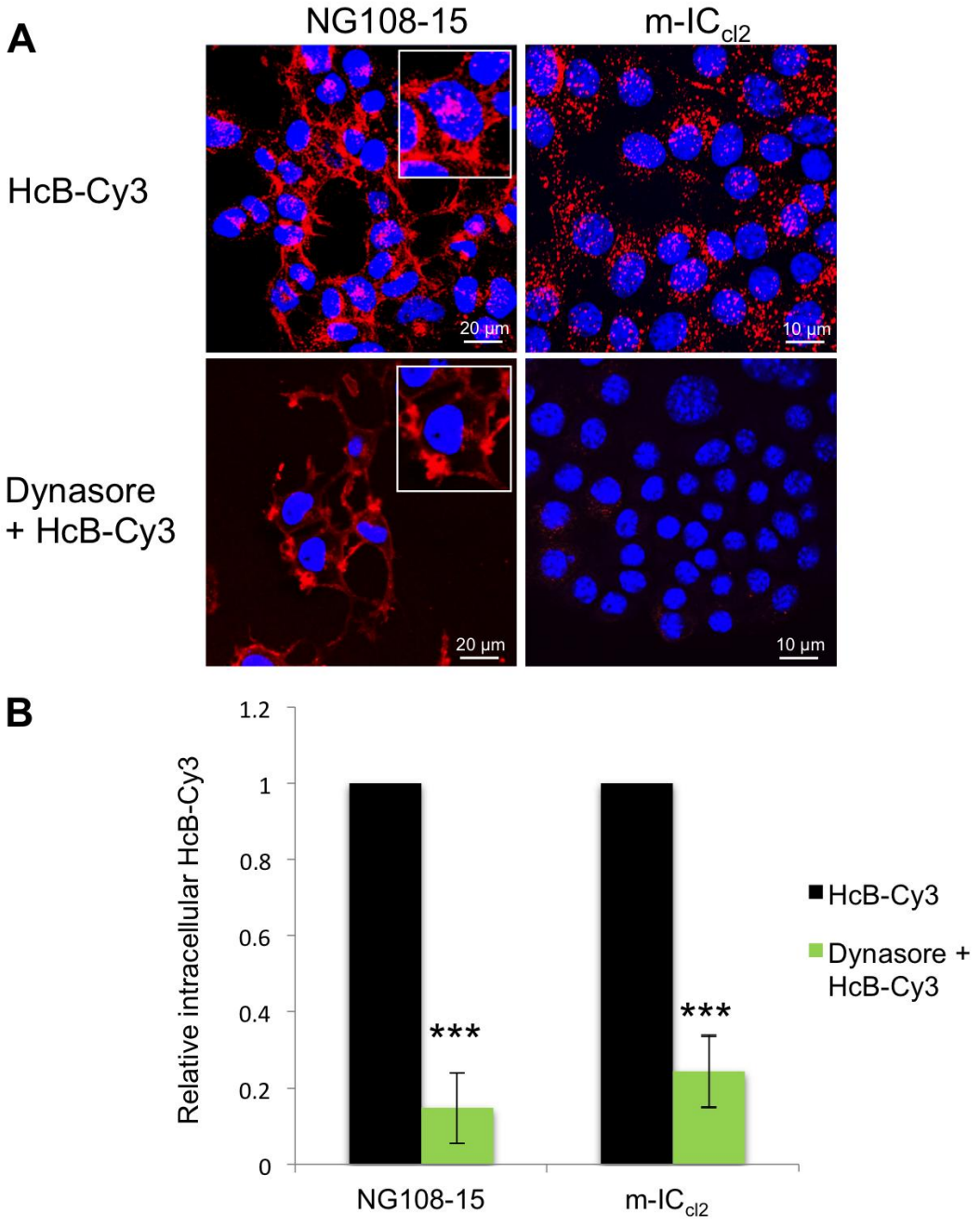


Figure 3. Inhibition of HcB-Cy3 entry into NG108-15 cells and intestinal crypt m-IC$_{cl2}$ cells by Dynasore.

(A) Cells plated on glass slides were pretreated with Dynasore 80 µM for 30 min at 37°C. Then, HcB-Cy3 (2.5 µg/ml) was added and cells were further incubated at 37°C for additional 10 min before being processed for microscopy.

This article is protected by copyright. All rights reserved.

(B) Quantification of HcB-Cy3 entry into control cells and cells pretreated with or without Dynasore. Fluorescence of intracellular HcB-Cy3 spots (in at least 20 cells from each of three independent experiments) was determined and the results were expressed as relative amounts of intracellular HcB-Cy3 in cells pretreated with Dynasore versus control cells. The level of internalized HcB-Cy3 in control NG108-15 or m-IC_{cl2} cells without Dynasore was arbitrarily assigned to 1. Data are mean values ± SD. Differences between means were tested using Student's *t*-test, and *p*-values <0.001 were taken to indicate significance (***).

Accepted Article

This article is protected by copyright. All rights reserved.

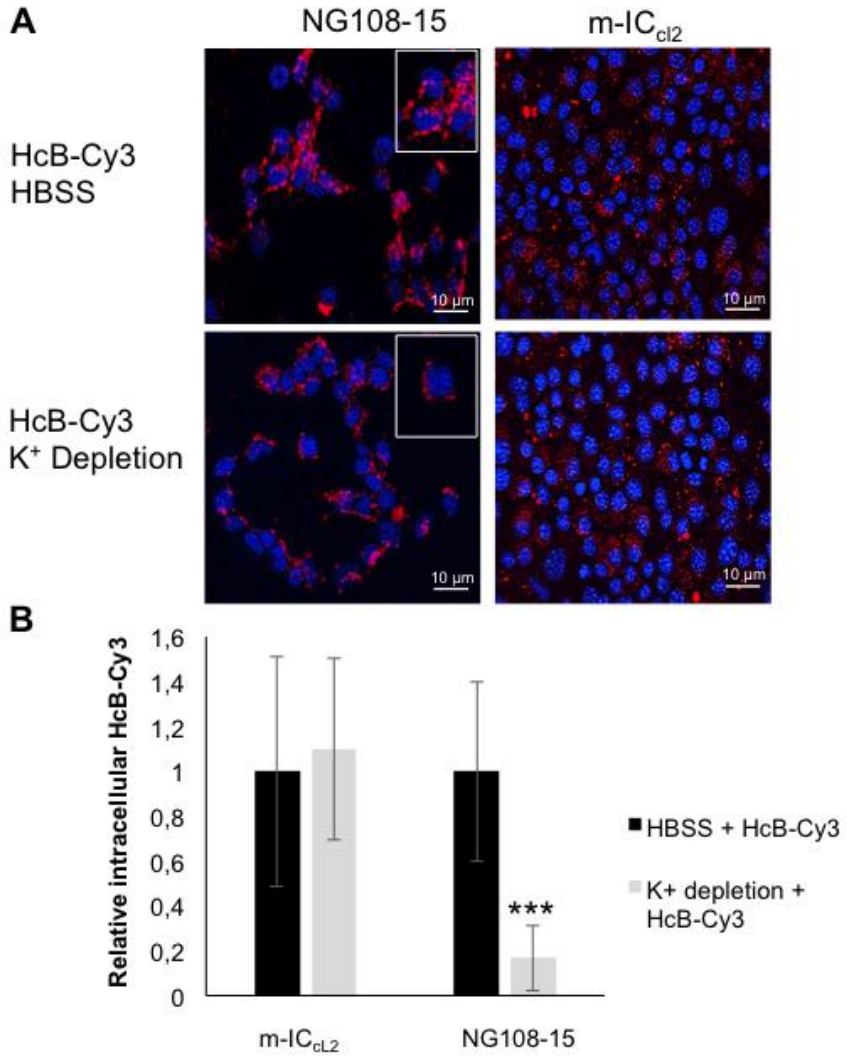


Figure 4. K+ depletion impairs HcB-Cy3 entry into NG108-15 and not in m-IC$_{cl2}$ cells. (A) Cells were incubated in K+ depleted buffer or in HBSS containing 10 mM KCl for 30 min at 37°C followed by a hypotonic shock of 5 min, and then exposed to HcB-Cy3 for additional 10 min. (B) Quantification of HcB-Cy3 entry in control cells and cells incubated in K+ depleted buffer as described in Fig. 3. The level of internalized HcB-Cy3 in control m-IC$_{cl2}$ cells was arbitrarily assigned to 1. Data are mean values ± SD from at least three independent experiments. Differences between means were tested using Student's *t*-test, and *p*-values <0.001 were taken to indicate significance (***).

This article is protected by copyright. All rights reserved.

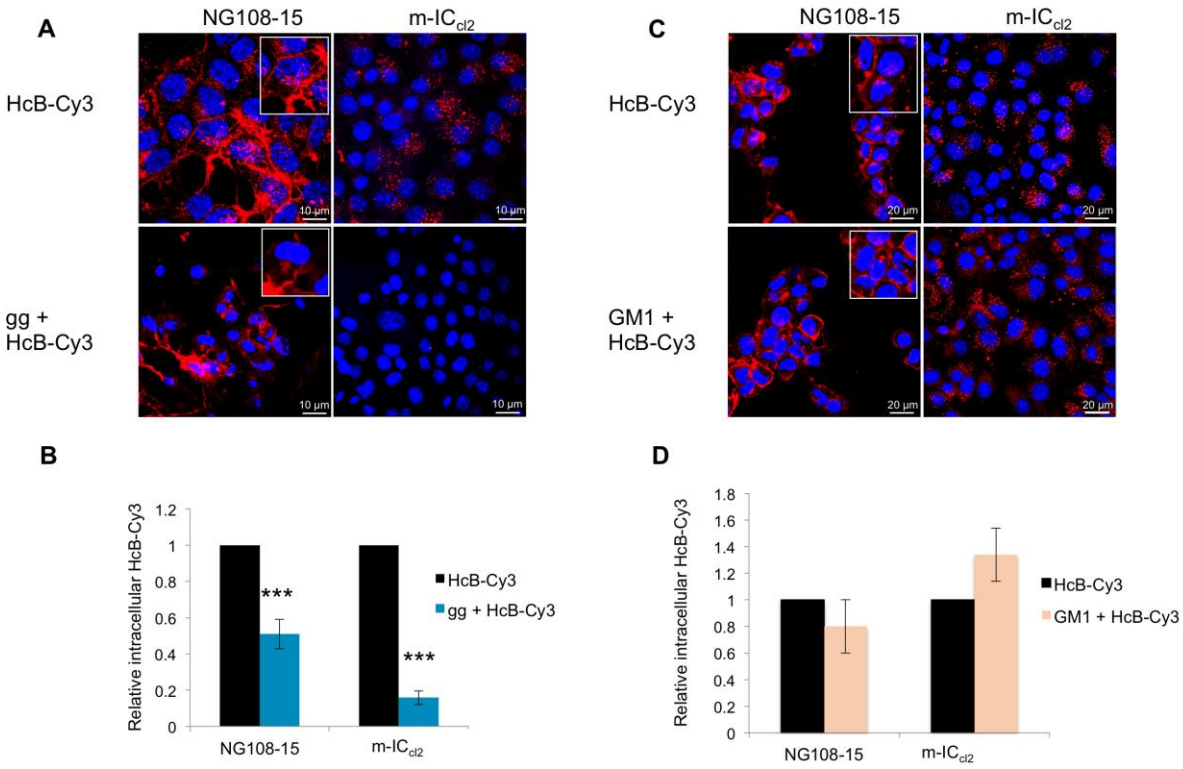


Figure 5. HcB-Cy3 entry into m-IC$_{cl2}$ cells is dependent of the gangliosides GD$_{1a}$, GD$_{1b}$, GT$_{1b}$ but not of GM1.

HcB-Cy3 (2.5 µg/ml) was preincubated with (A) a preparation (gg) enriched in gangliosides (18% GM1, 55% GD$_{1a}$, 15% GD$_{1b}$, 10% GT$_{1b}$, 2% others; 250 µg/ml), or (C) GM1 (50 µg/ml), for 30 min at room temperature. Then, the mix was added to NG108-15 cells or m-IC$_{cl2}$ cells plated on glass cover slides, and the cells were incubated for additional 10 min at 37°C before being processed for microscopy.

Quantification of HcB-Cy3 entry in untreated cells and cells pretreated with gg (B) or GM1 (D) was performed as described in Fig. 3. The level of internalized HcB-Cy3 in control NG108-15 or m-IC$_{cl2}$ cells was arbitrarily assigned to 1. Data are mean values ± SD from at least three independent experiments. Differences between means were tested using Student's *t*-test, and *p*-values <0.001 were taken to indicate significance (***).

Accepted

This article is protected by copyright. All rights reserved.

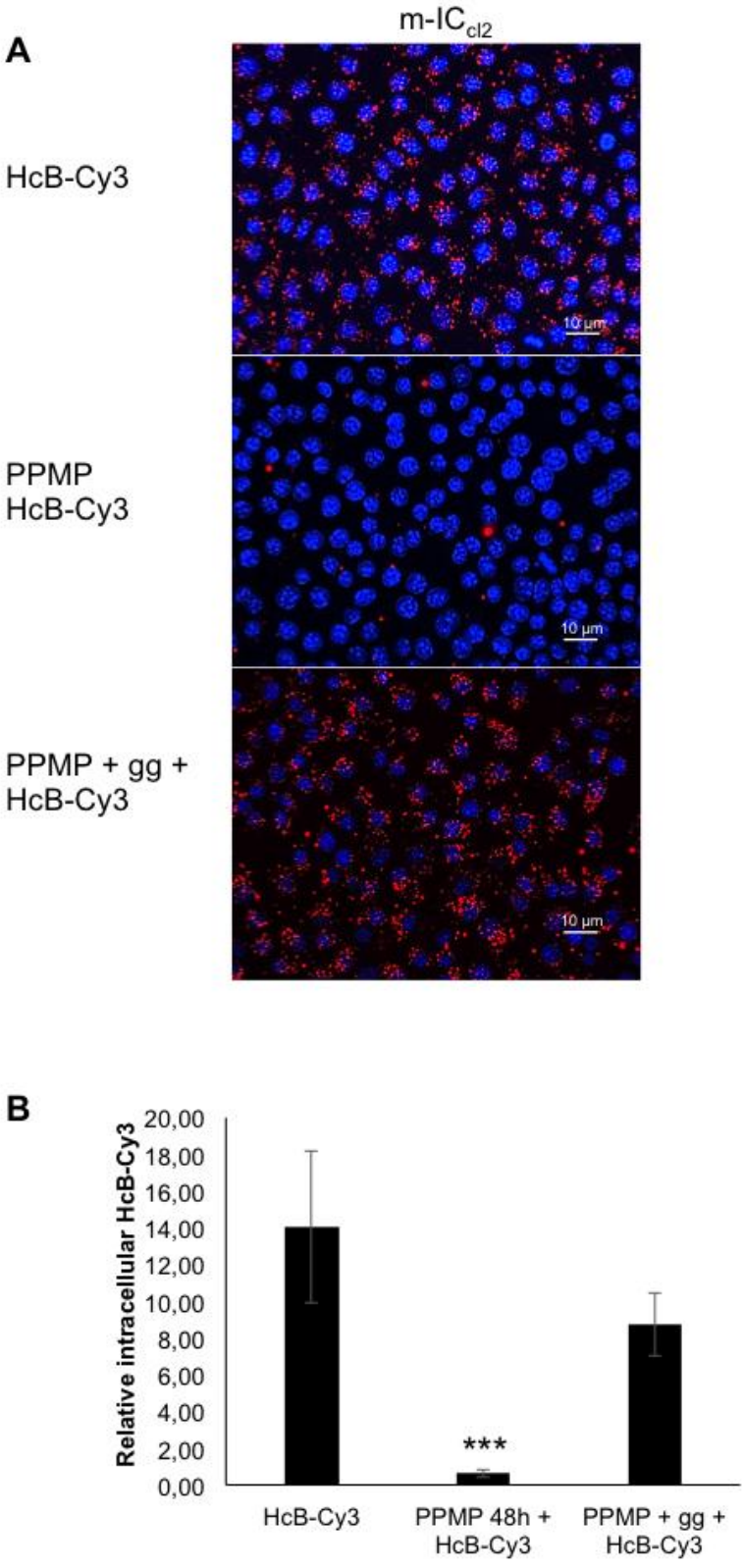


Figure 6. Inhibition of ganglioside synthesis impairs HcB-Cy3 entry into m-IC$_{cl2}$ cells. (A) Untreated cells and cells treated with PPMP (7.5 µg/ml) for 48 h were exposed to HcB-Cy3 (2.5 µg/ml) for 10 min. For ganglioside complementation, the cells treated with PPMP for 24

This article is protected by copyright. All rights reserved.

h were supplemented with the mixture of gangliosides enriched in GD_{1a}, GD_{1b}, and GT_{1b} (250 μg/ml) (PPMP + gg). (B) Quantification of HcB-Cy3 entry in untreated cells and cells pretreated with PPMP or PPMP + gg was performed as described in Fig. 3. The level of internalized HcB-Cy3 in control m-IC_{cll} cells was arbitrarily assigned to 1. Data are mean values ± SD from at least three independent experiments. Differences between means were tested using Student's *t*-test, and *p*-values <0.001 were taken to indicate significance (***).

Accepted Article

This article is protected by copyright. All rights reserved.

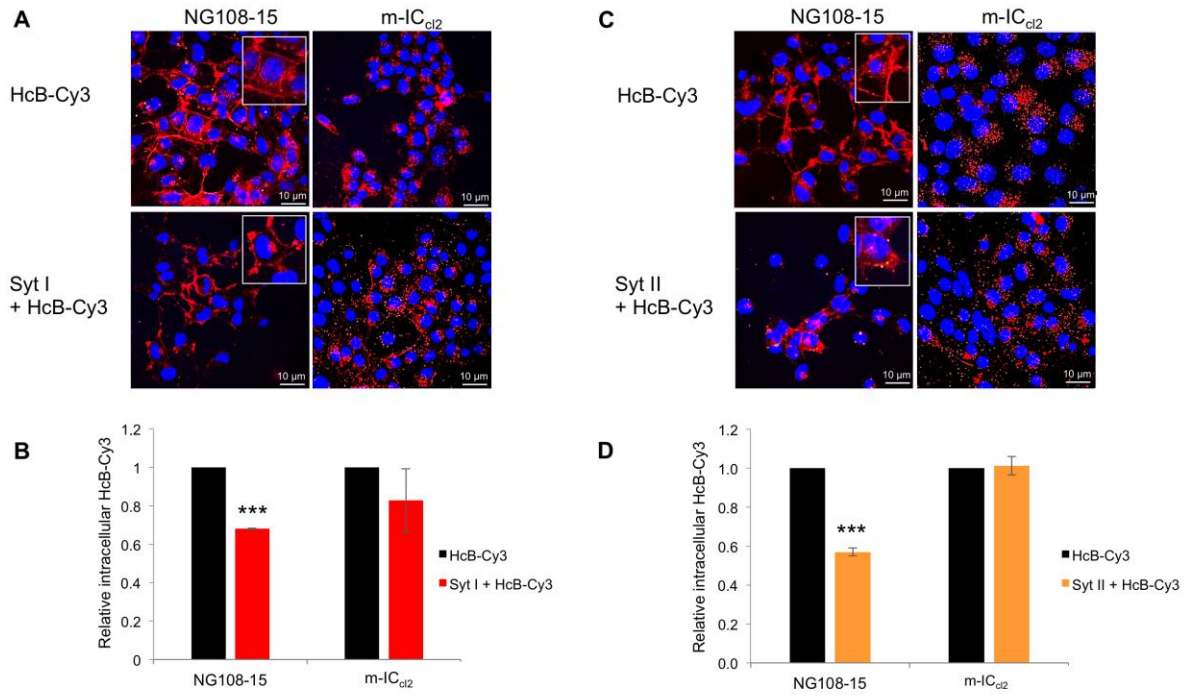


Figure 7. HcB-Cy3 entry into m-IC$_{cl2}$ cells is not dependent of synaptotagmin (Syt) I and II.

HcB-Cy3 (2.5 µg/ml) was preincubated with the recombinant domain of (A) SytI or (C) SytII (25 µg/ml) for 30 min at room temperature. Then the mix was added to NG108-15 cells or m-IC$_{cl2}$ cells plated on glass cover slides and the cells were incubated for additional 10 min at 37°C before being processed for microscopy.

HcB-Cy3 entry was quantified in control cells and cells pretreated with SytI (B) or SytII (D) as described in Fig. 3. Data are mean values ± SD from at least three independent experiments. Differences between means were tested using Student's *t*-test, and *p*-values <0.001 were taken to indicate significance (***).

Accepted Article

This article is protected by copyright. All rights reserved.

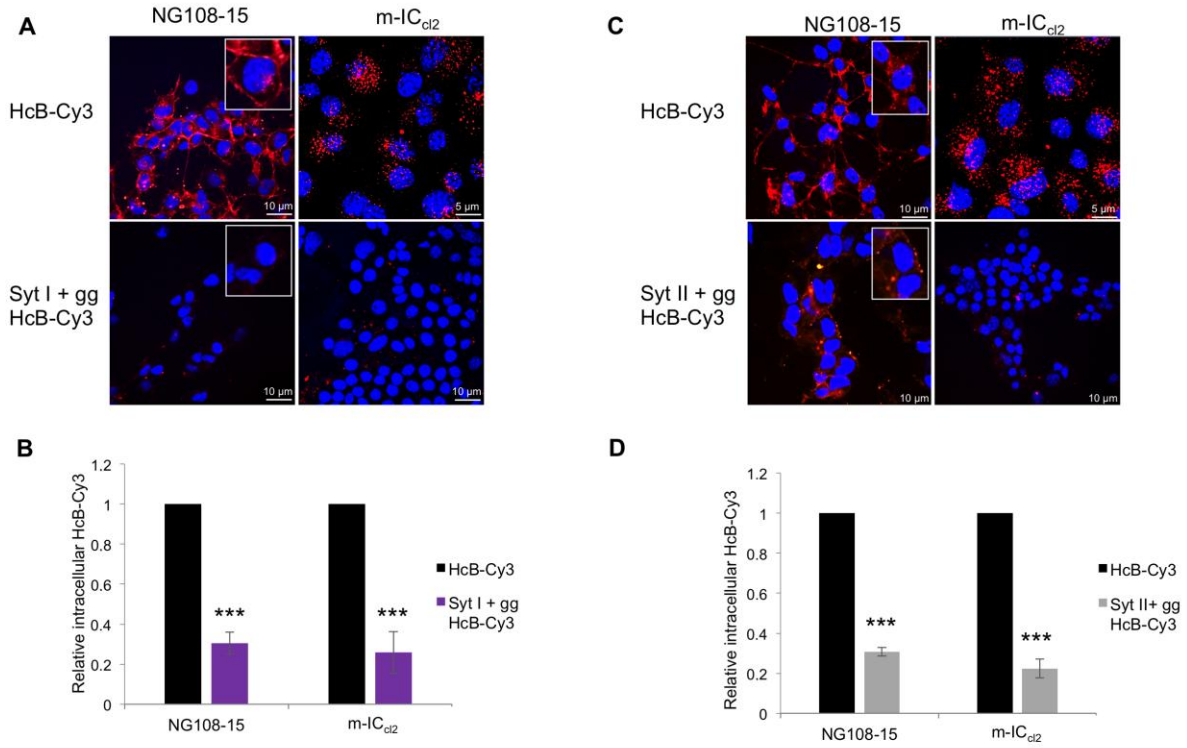


Figure 8. Both gangliosides (GD_{1a}, GT_{1b}) and synaptotagmin are required for HcB entry into neuronal cells.

HcB-Cy3 (2.5 µg/ml) was preincubated with both a preparation (gg) enriched in gangliosides (18% GM1, 55% GD_{1a}, 15% GD_{1b}, 10% GT_{1b}, 2% others; 250 µg/ml) and the recombinant domain of (A) SytI or (C) SytII (25 µg/ml) for 30 min at room temperature. Then the mix was added to NG108-15 cells and m-IC_{cl2} cells plated on glass cover slides, and the cells were incubated for additional 10 min at 37°C before being processed for microscopy.

HcB-Cy3 entry was quantified in control cells and cells pretreated with gg and SytI (B) or gg and SytII (D) as described in Fig. 3. Data are mean values ± SD from at least three independent experiments. Differences between means were tested using Student's *t*-test, and *p*-values <0.001 were taken to indicate significance (***).

This article is protected by copyright. All rights reserved.

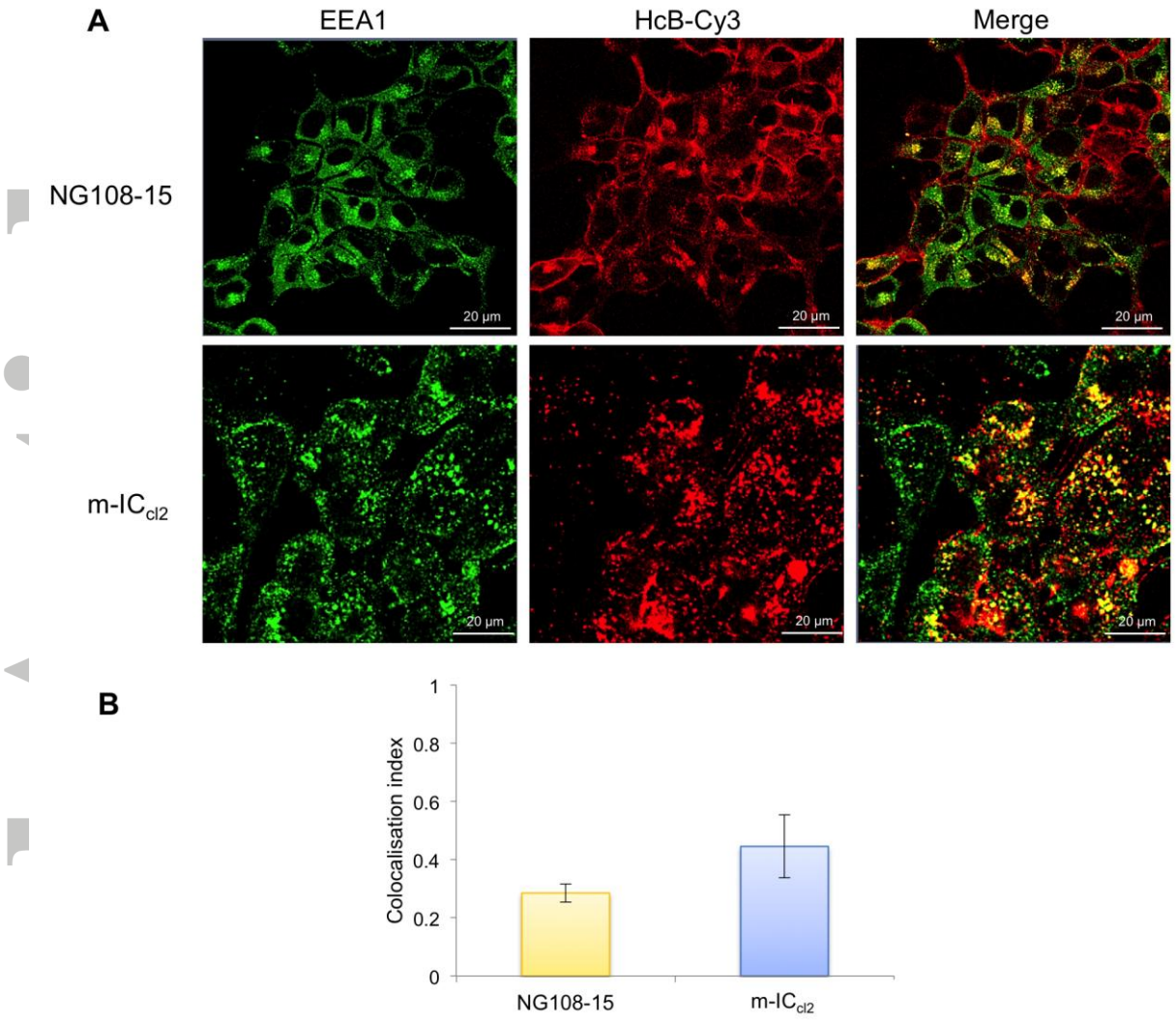


Figure 9. HcB-Cy3 enters NG108-15 and m-IC$_{cl2}$ cells through early endosomes. A) HcB-Cy3 (2.5 µg/ml) was incubated with NG108-15 cells or m-IC$_{cl2}$ cells plated on glass slides for 10 min at 37°C. Then, the cells were fixed, permeabilized, and stained with antibodies against endogenous EEA1.

B) Quantification of colocalization between HcB-Cy3 and anti-EEA1. Colocalization index was determined as Pearson's coefficient. The distribution of cell structures recognized by HcB-Cy3 was expressed as the ratio of the number of cell structures co-stained with HcB-Cy3 and anti-EEA1 to the total of cell structures labeled with anti-EEA1. The mean values ± SD of the Pearson's correlation coefficient of 20-30 cells from at least three independent experiments are shown.

Accept

This article is protected by copyright. All rights reserved.

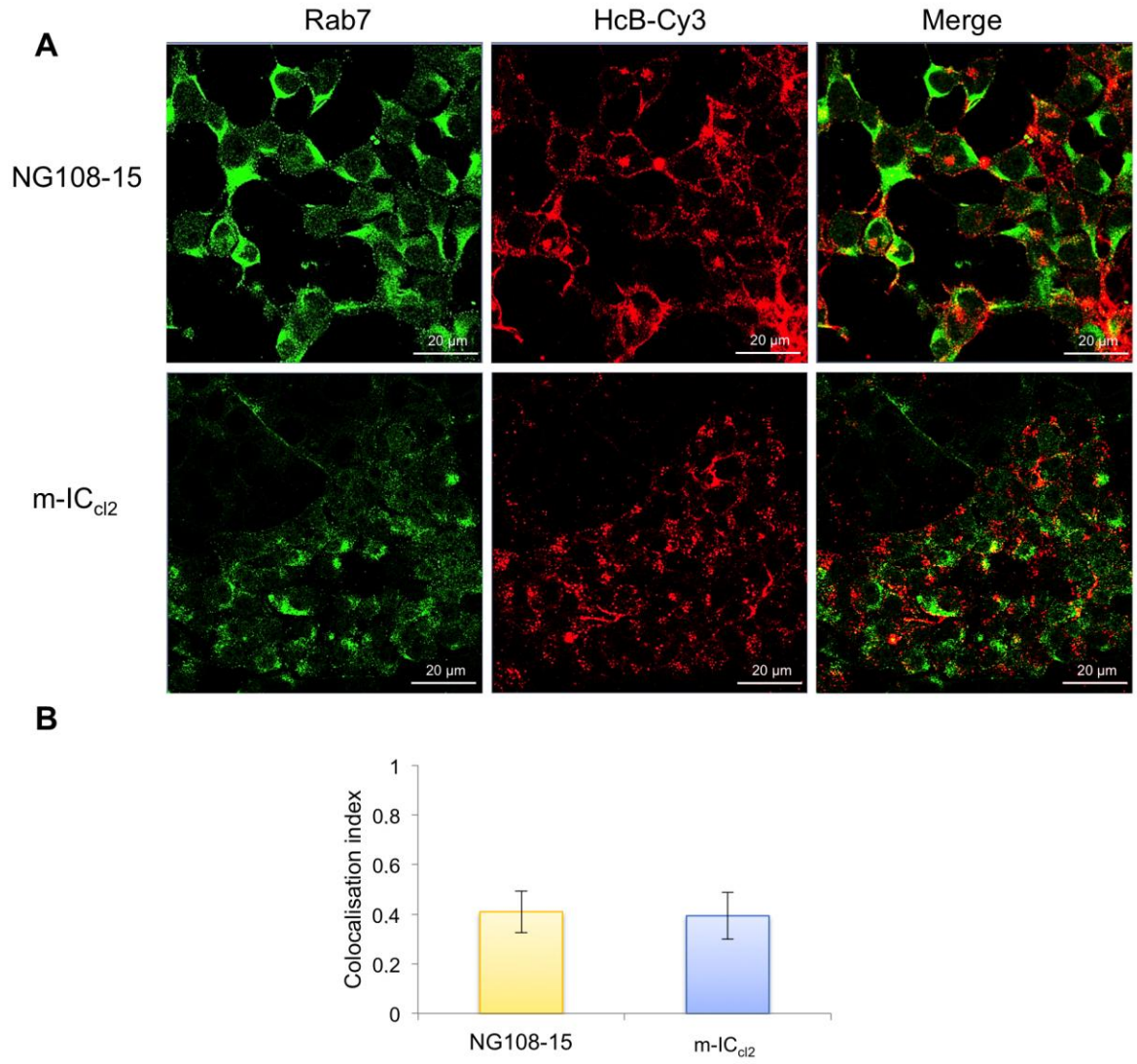
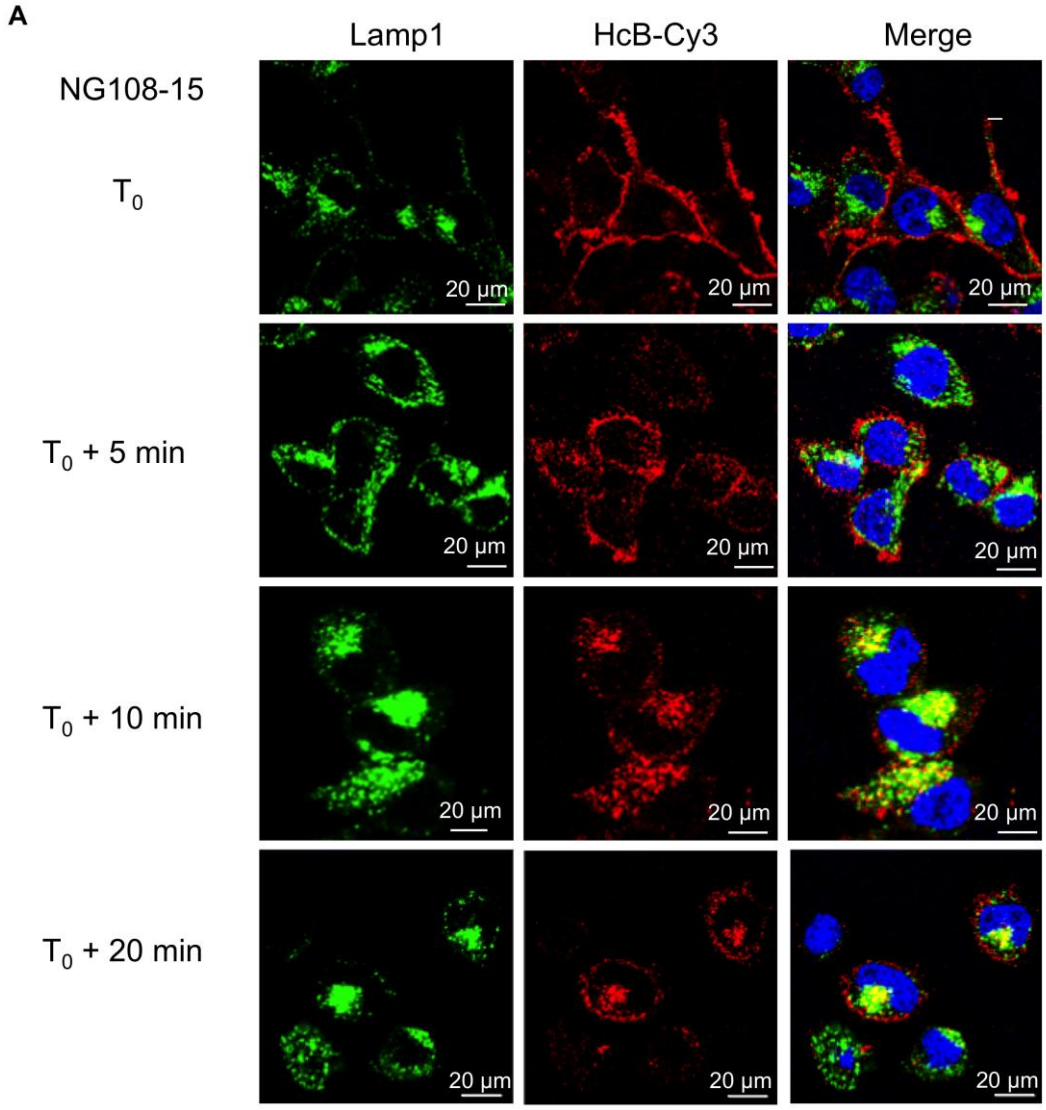


Figure 10. HcB-Cy3 enters NG108-15 cells and m-IC$_{cl2}$ cells through an early Rab7 compartment. A) HcB-Cy3 (2.5 µg/ml) was incubated with NG108-15 or m-IC$_{cl2}$ cells plated on glass slides for 10 min at 37°C. Then, the cells were fixed, permeabilized, and stained with antibodies against Rab7.

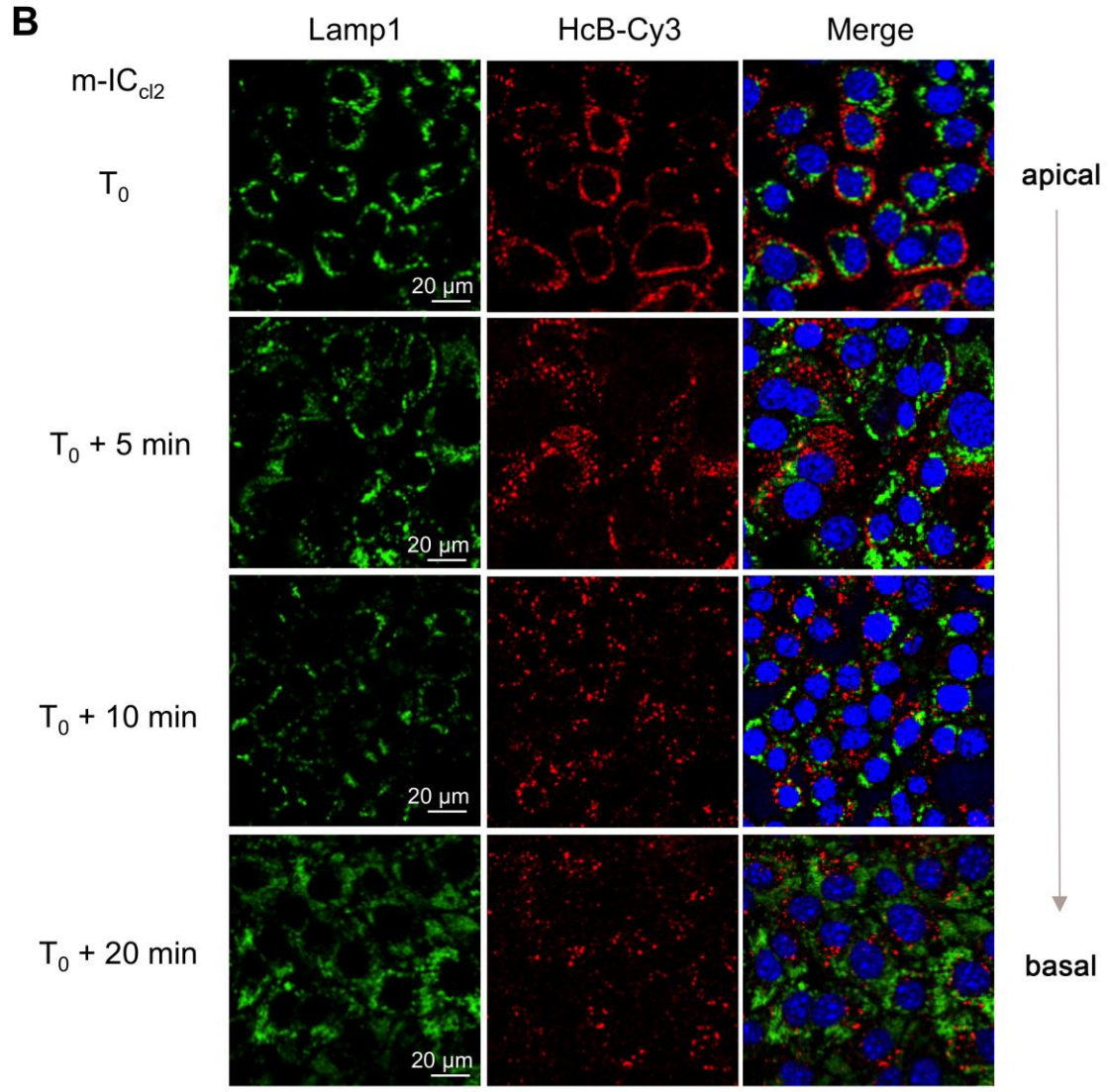
B) Quantification of colocalization between HcB-Cy3 and anti-Rab7. Colocalization index was determined as Pearson's coefficient. The distribution of cell structures recognized by HcB-Cy3 was expressed as the ratio of the number of cell structures co-stained with HcB-Cy3 and anti-Rab7 to the total of cell structures labeled with anti-Rab7. The mean values ± SD of the Pearson's correlation coefficient of 20-30 cells from at least three independent experiments are shown.

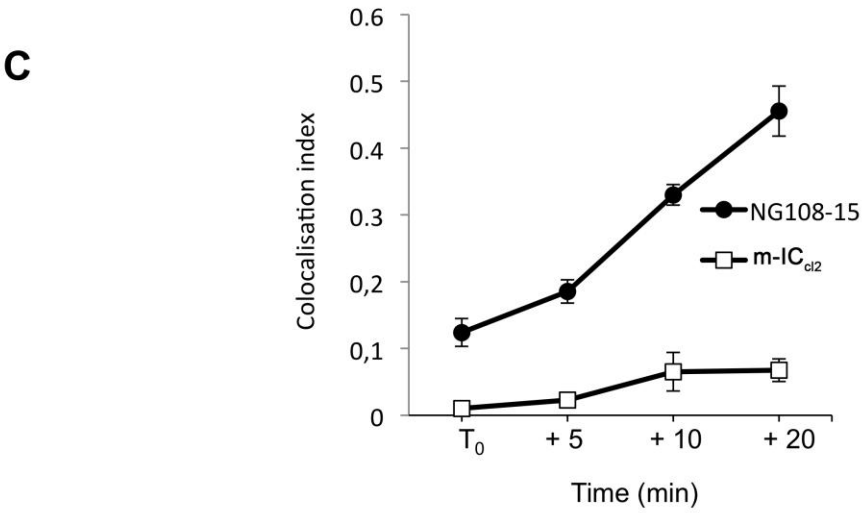
This article is protected by copyright. All rights reserved.



Accep

This article is protected by copyright. All rights reserved.





This article is protected by copyright. All rights reserved.

Figure 11. Differential HcB-Cy3 trafficking through late endosomes in NG108-15 cells compared to m-IC$_{cl2}$ cells. A) NG108-15 cells plated on glass slide were incubated with HcB-Cy3 (2.5 µg/ml) for 3 min at 37°C. Then, the culture medium was replaced with Dulbecco's medium. The cells were further incubated at 37°C for the indicated times, and were fixed, permeabilized, stained with antibodies against Lamp1, and processed for confocal microscopy.

B) HcB-Cy3 (2.5 µg/ml) was incubated in the apical chamber of polarized m-IC$_{cl2}$ cells grown on filters for 3 min at 37°C. Then, the culture medium was replaced with Dulbecco's medium. The cells were further incubated at 37°C for the indicated times, and were fixed, permeabilized, stained with antibodies against Lamp1, and processed for confocal microscopy. Representative plans from apical to basolateral side overtime are shown.

C) Quantification of colocalization between HcB-Cy3 and anti-Lamp1. Colocalization index was determined as Pearson's coefficient. The distribution of cell structures recognized by HcB-Cy3 was expressed as the ration of the number of cell structures co-stained with HcB-Cy3 and anti-Lamp1 to the total of cell structures labeled with anti-Lamp1. The mean values ± SD of the Pearson's correlation coefficient of 20-30 cells from at least three independent experiments are shown.

Accepted Article

This article is protected by copyright. All rights reserved.

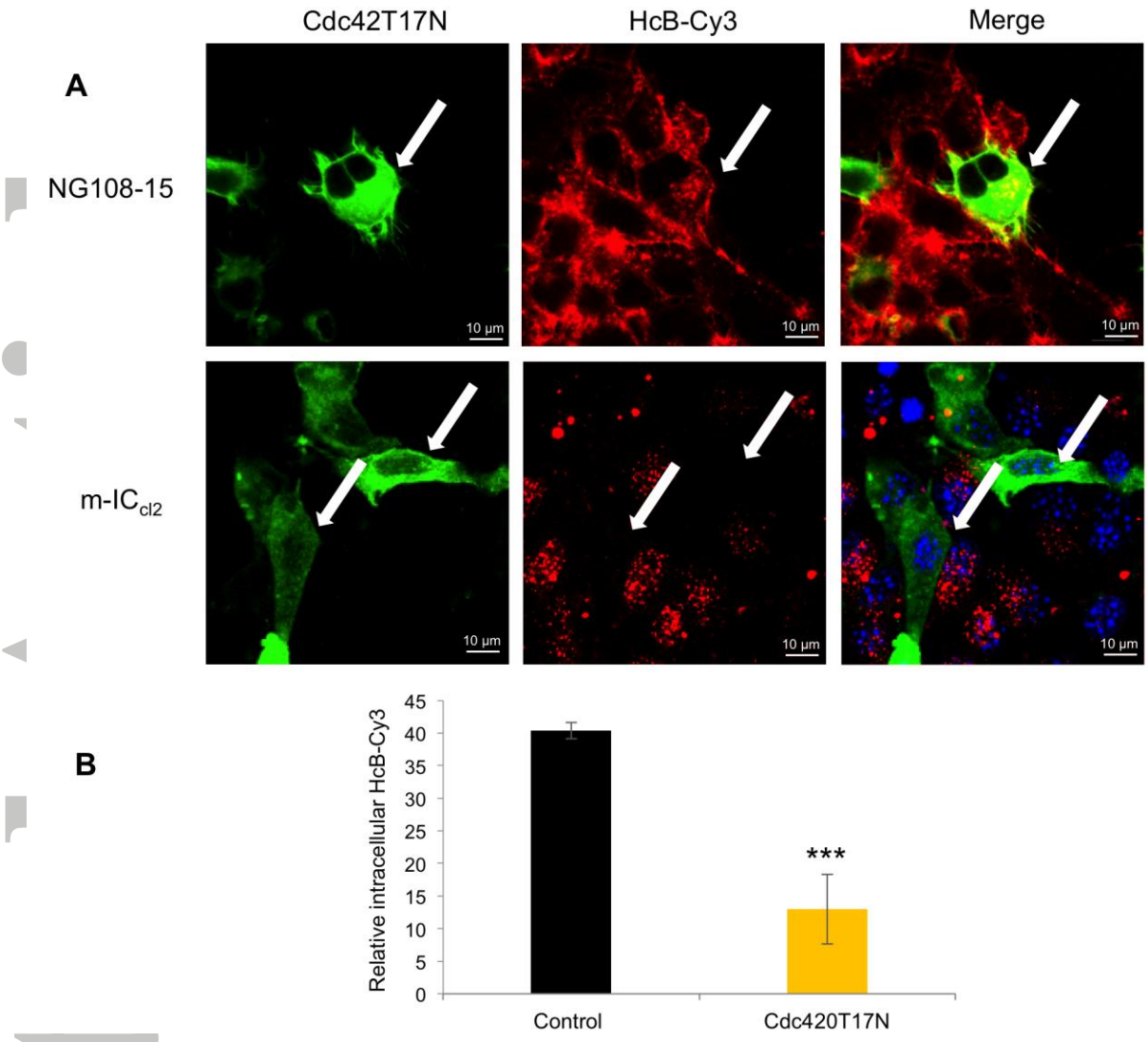


Figure 12. HcB-Cy3 entry is Cdc42 dependent in intestinal m-IC$_{cl2}$ cells but not in neuronal NG108-15 cells. A) m-IC$_{cl2}$ cells were transfected with a plasmid encoding GFP-Cdc42T17N and plated on glass slide. The cells were incubated with HcB-Cy3 (2.5 µg/ml) for 10 min at 37°C, and then were processed for confocal microscopy. Arrows indicate transfected Cdc42T17N cells.

B**)** Quantitative analysis of HcB-Cy3 entry into cells overexpressing Cdc42 dominant negative (Cdc42T17N) was performed by counting the total number of vesicles containing HcB-Cy3 in several cells (n > 40) and in different fields obtained from at least three independent experiments. The mean values were determined for both transfected cells and non-transfected (control) cells. Data are expressed as the mean ratio ± SD between non-transfected or transfected cells versus total number of cells. Differences between means were tested using Student's *t*-test, and *p*-values <0.001 were taken to indicate significance (***).

This article is protected by copyright. All rights reserved.